Master's thesis

2019

Jonas Okstad

NTNU
Norwegian University of
Science and Technology
Faculty of Engineering
Department of Mechanical and Industrial Engineering

Jonas Okstad

Modelling and Analysis of Electrical Field Gradients over Offshore Pipelines with Cathodic Protection

Impact of Drain to Subsea Wells

June 2019

NTNU
Norwegian University of
Science and Technology

NTNU
Norwegian University of
Science and Technology

NTNU

Norwegian University of
Science and Technology

Modelling and Analysis of Electrical Field Gradients over Offshore Pipelines with Cathodic Protection

Impact of Drain to Subsea Wells

Jonas Okstad

Materials Science and Engineering
Submission date: June 2019
Supervisor: Roy Johnsen
Co-supervisor: Gro Østensen Lauvstad
Harald Osvoll

Norwegian University of Science and Technology
Department of Mechanical and Industrial Engineering

Preface

This master's thesis is submitted to Norwegian University of Science and Technology (NTNU) as the final work of the master's degree program Materials Science and Engineering at the department of Mechanical and Industrial Engineering. The project has been a collaboration between NTNU and Force Technology Norway AS, with Roy Johnsen as the main-supervisor together with Gro Østensen Lauvstad and Harald Osvoll as co-supervisors from Force Technology. Magnus Myhr from Force Technology has also participated in meetings, provided input and comments on results, and most important, given guidance regarding modelling issues during the project.

Acknowledgement

My gratitude goes to Roy Johnsen for his expertise as a supervisor and guidance throughout the project period. I would like to thank my co-supervisors, Gro Østensen Lauvstad and Harald Osvoll for guidance and continuous feedback during the work of the project. Your knowledge has been valuable and of great help.

In addition, I will give attention to Magnus Myhr. I'm forever grateful for his help regarding modelling and also for always being available and interested in discussing project related issues. He has been an important part of this project and been a great supporter. Thank you.

Trondheim, June 11, 2019

Jonas Okstad

Abstract

The oil and gas industry is one of the most important industries to the Norwegian economy, but the industry also has an enormous responsibility when it comes to the consequences of failure of offshore pipelines and structures. Cathodic Protection (CP) is one of the most effective methods for decreasing the corrosion of structures and pipelines and hence reducing the risk of oil and gas leakage due to corrosion failure. Subsea wells are not considered critical object that require cathodic protection per design, but a current drain to these structures are added to the CP design of adjacent structures and pipelines to compensate for the protection of these structures. The effect subsea wells have on adjacent CP systems is not well investigated and a limited amount of studies investigate how much current subsea wells drains and how this current drain evolves over time.

In this study, improving the understanding of the behaviour of subsea wells and how current is drained from the CP systems of adjacent pipelines is of interest. Real field data from a known subsea field, referred to as Field A, is used as a reference to build a realistic model where the measured anode current output is matched as good as possible by simulated drain profiles. There are several unknown parameters that is necessary to create such a model, as the geometrical parameters of the well structure, i.e. the depth, radius and number of wells. A parameter study is performed to investigate the importance of these parameters and how they affect the drain profile of the pipeline's anodes. Comsol Multiphysics is used as modelling software, and several models are created to investigate the effect of the parameters, to compare the simulated and measured drain profile and to verify the results from the comparison.

The results from the parameter study show that neither of the geometrical parameters of the well structure affect the percentage amount of anode current output of the total current drained, which means that the value of these parameters is not critical to obtain a realistic, simulated drain profile. The result of the modelling where all aspects regarding drain is included, as drain from both adjacent pipelines to the drain point and the drain from the template structure, show that the simulated drain profile matches the measured drain profile well. The same conclusion can be made from the verification model, and hence the model can be used as a tool to investigate other CP problems regarding current drain to subsea wells.

Sammendrag

Olje- og gassindustires er en av de viktigste industriene for norsk økonomi, men denne industrien har også et enormt ansvar når det kommer til konsekvensene av svikt av offshorestrukturer og -rørledninger. Katodisk Beskyttelse er en av de mest effektive metodene for å redusere sjansen for korrosjon av strukturer og rørledninger and er dermed risikoen for olje- og gasslekkasje på grunn av svikt som følge av korrosjon. Undervannsbrønner er ikke antatt å være kritiske strukturer som trenger egen katodisk beskyttelse, men strømdrenasje til brønner legges til designet av omliggende rørledninger og strukturer for å kompensere for strømmen brønner drenerer fra andre beskyttelsessystemer. Effekten av strømdrenasje fra omliggende beskyttelsessystemer er ikke i stor grad undersøkt og et fåtall studier tar for seg hvor mye strøm som dreneres til brønner og hvordan dette endrer som over tid.

I denne studien er målet å forbedre forståelsen av hvordan strøm dreneres til undervannsbrønner og hvor mye som faktisk dreneres. Reelle feltdata fra et kjent felt, referert til som Felt A, er brukt som referanse til å lage en modell hvor målt og simulert strømdrenasje skal sammenlignes. Flere parametere som er nødvendig for å lage modellen er ukjent, hvor fleste av disse er parametere som beskriver geometrien til brønnen. En parameterstudie er derfor gjort for å finne effekten av disse parameterne og om de er viktige for å lage en modell som fungerer. Comsol Multiphysics er dataprogrammet som er brukt til modelleringen, og flere modeller er lagd for å både se effekten av parameterne og får å validere resultatene som er oppnådd.

Resultatene fra parameterstudiet viser at ingen av de geometriske parameterne har noen effekt på prosentvis mengde strøm som hver anode leverer til drenasje, som betyr at geometrien på brønnen ikke er kritisk for å oppnå en realistisk, simulert drenasjeprofil. Resultatene fra modellen hvor alle aspekter med tanke på drenasje til brønn er inkludert, som drenasje fra begge nærliggende rørledninger og drenasje fra beskyttelsesstruktur, viser at den simulerte drenasje profilen stemmer godt over ens med den målte. Den samme konklusjonen kan bli gjort når det kommer til modellen hvor disse resultatene valideres, hvor det samme resultatet blir oppnådd, noe som vil si at modellen fungerer og kan benyttes til å studere andre problemer knyttet til strømdrenasje til undervannsbrønner.

Table of Content

List of Figures

List of Tables

Abbreviations

Nomenclature

A	Amps
BC	Boundary Condition
BEM	Boundary Element Method
CCD	Constant Current Density
CP	Cathodic Protection
DOB	Depth of Burial
FDM	Finite Difference Method
FEM	Finite Element Method
GDP	Gross Domestic Product
ICCP	Impressed Current Cathodic Protection
NCS	Norwegian Continental Shelf
PDCD	Potential Dependent Current Density
ROV	Remotely Operated Vehicle
SA	Sacrificial Anode
SACP	Sacrificial Anode Cathodic Protection
V	Volts

Symbols

I	Total Current
I_0	Exchange Current
I_{corr}	Corrosion Current
ϕ	Electrode Potential
ϕ_0	Equilibrium Potential
ϕ_{corr}	Corrosion Potential
$\partial\phi$	Variation in potential
α	Electric transfer coefficient
β	Tafel slope

β_a Anodic Tafel slope

β_c Cathodic Tafel slope

η Overpotential

κ Electrolyte Conductivity

Γ Boundary enclosing the Laplace volume

Ω Laplace volume

J Unidirectional flux

D Diffusion Coefficient

∂x Variation in distance

z Electric charge

F Faraday's number

R Gas constant

T Absolute temperature

C Bulk concentration

∂C Variation of concentration

v Velocity

1 Introduction

1.1 Background

The oil and gas industry have been, and still is one of the most important industries for the Norwegian economy, and since the first discovery of oil and gas on the Norwegian Continental Shelf (NCS), petroleum production has added more than NOK 9000 billon to the Norwegian Gross Domestic Product (GDP) [1]. Such a large industry comes with a lot of responsibility, to maintain the safety for the environments surrounded by offshore platforms and a network of pipelines at the seabed by preventing oil and gas leakage. Corrosion of these structures is a dangerous factor that may cause detrimental emissions of oil and gas which has to be prevented. The use of CP of these platforms and pipelines can be a cost-effective solution to prevent severe external corrosion when the structures are exposed to an aggressive environment such as seawater [2].

A CP system is designed according to standard, as DNVGL-RP-B401 [4], NORSOK M-503 [6] and ISO 15589-2 [7]. Several parameters have to be considered when a CP system is designed, as design life required, pipe diameter and length, geographic location, type of coating, installation method, water depth, burial method of the pipeline, production temperature and environment temperature and electrical isolation from platforms or other pipelines [3]. Even though a CP system is well designed according to different standards and fulfils all the necessary requirements, the CP system has to be periodically inspected to verify that the system is working as it should and to assess the remaining lifetime of the sacrificial anodes (SA). Pipeline inspection has been performed for decades and is still under development to find new and better methods to obtain as much information as possible from a CP system. The gathered information from an inspection have to go through a post-processing process where the data are evaluated in combination with the use of software modelling.

1.2 Problem Description

Related to cathodic protection of pipelines, an electric field is created due to the current that is transferred between anodes and cathode, i.e. bare steel. Variations in this electrical field is an indication of the strength and the direction of the current that flows in the electrolyte. Through literature and theory, this electrical field and how it is affected should be described. The purpose of this thesis is to improve the understanding regarding the electrical field surrounding the pipelines. In addition, measurement methods for pipeline surveys, respectively potential and field gradient based surveys, should be compared. The thesis should also enlighten results from surveys performed by FiGS®, a sensor developed by Force Technology AS for field gradient measurements.

1.3 Project Scope

1.3.1 Research Questions

This master's thesis had one question of interest, that the whole study is built upon: "Is it possible to find a general polarization curve that can be used as boundary condition on a well surface that reflects the current it drains from a pipeline's CP system?".

1.3.2 Objectives

The objective for this master thesis is a continuation of the project thesis done in the autumn of 2018. Several problems regarding CP modelling of offshore pipelines are investigated, where the investigation of current drain to subsea wells are in focus. During the modelling, boundary conditions for anode and cathode surface and the effect of buried anodes are also investigated.

The models developed are based on pipelines from a field where a FiGS® survey has been performed and the measured data are used as reference and compared to the simulated data. The main goal of the thesis is to create a model where a pipeline including anodes and subsea wells are defined as realistic as possible regarding input parameters and a simulated drain profile that reflects a drain profile obtained by FiGS® survey is the result.

To obtain a simulated drain profile that matches the reference profile, the effect of the well geometry has to be investigated to study the importance of the geometrical parameters as the well depth, the well casing radius and the number of wells in the drain point. The cathodic

boundary conditions, as the polarization curve is also investigated, to determine the effect it has on the drain to the well casings.

1.3.3 Limitations

During the development of the models, several assumptions have been made due to lack of information regarding the geometry of the wells. However, these assumptions have not been critical for the results.

The pipelines had been in service for eight years at the time of the survey, which means that the data obtained from the survey may deviate from data obtained from a survey right after installation due to anode consumption, coating degradation and calcareous deposits. The anode consumption is affected by the coating degradation and calcareous deposits formed during the service life. The data obtained from the simulations is valid for new anodes, which will be a source of error since the simulated data are not compared to survey data at the same stage of time.

1.4 Thesis Structure

This master's thesis is mainly divided into a theoretical background, literature review, numerical modelling, modelling results, discussion and conclusion. A chapter where further work is suggested is also included.

The theoretical background describes the different important aspects of computer modelling, where the different methods and the equations to be solved for CP problems are described. Basic information regarding corrosion and CP is also included briefly.

The literature review focuses on some different important aspects that have to be considered modelling a CP problem.

The modelling chapter, which can be compared to an experimental chapter, describes the modelling procedure, the geometry and the boundary conditions. In the procedure, the different cases are described and also important aspects that have to be considered building the models.

The results of interest are visualized as a drain profile, where the anode current output for each anode is plotted as a function of their position.

In addition to discuss the effect and importance of the results in light of current drain, applications of the model as a tool to investigate CP problems related to current drain is also discussed.

2 Theoretical Background

2.1 Cathodic Protection

2.1.1 Basics of Corrosion

Steel has been the only economically favourable material for offshore pipelines used for transportation of oil and gas, but with a major disadvantage, the lack of corrosion resistance of carbon steel in aggressive environments as seawater. The consequences related to pipeline failure due to corrosion require that CP systems are used to avoid corrosion on the outer pipe surface and that these systems are maintained such that they are as reliable as possible [8]. The corrosion of the steel in seawater is an electrochemical process and is represented as an oxidation reaction. The reduction reaction occurs at the surface of the steel. Oxidation of iron is the anodic reaction and can be described as *reaction 2.1*. For *reaction 2.1* to occur, a simultaneous reaction involving consumption of the electrons have to be present, which is the reduction reaction.

$$Fe(s) = Fe^{2+} + 2e^{-} \quad (2.1)$$

In seawater, the possible reduction reactions are:

$$2H^{+} + 2e^{-} = H_2 \quad (2.2)$$

$$2H_20 + 2e^{-} = H_2 + 2OH^{-} \quad (2.3)$$

$$O_2 + 2H_20 + 4e^{-} = 4OH^{-} \quad (2.4)$$

$$O_2 + 4H^{+} + 4e^{-} = 2H_20 \quad (2.5)$$

Reaction 2.4, which is the most likely oxygen reduction reaction to occur (ORR), is the formation of hydroxide ions, and these ions can react with the iron (II) ions leading to the formation of rust, also known as Fe_2O_3. The formation of rust on unprotected steel in the presence of air and water cannot be avoided due to the electrochemical process that occurs spontaneously. To avoid the formation of rust and corrosion of steel, a potential more negative than – 0.8 V vs Ag/AgCl [7] have to be maintained at the steel surface. Steel itself has an open circuit potential of – 0.6 V vs Ag/AgCl [2], and a shift in potential to more negative values is

called polarization. Such polarization of the steel is achieved using a protection system. The most commonly used protection systems are coating, combined with sacrificial anode CP (SACP) or impressed current CP (ICCP) [9, 10].

2.1.2 Cathodic Protection

CP systems are used to polarize the cathode by supplying electrons as a protective current and coating is used to reduce the cathodic surface area and hence the current demand [9]. The use of galvanic SA creates a galvanic coupling between the steel and the anode, and the anode sacrifice itself to prevent corrosion of the steel. The reason why the anodes corrode instead of the steel is because the anode material has a more negative open circuit potential compared to steel. With a more negative potential, the anodes are less noble and will act as anode rather than the steel. The most commonly used anode materials for marine applications are Al and Zn alloys [10].

2.1.3 Calcareous Deposits

When SACP or ICCP systems are used, the reduction reaction on the cathode, i.e. the steel surface, results in the formation of hydroxide ions which changes the local pH in the electrolyte at the cathode surface. Carbon dioxide and water react and form carbonate ions at the cathode surface by the following reactions [11]:

$$CO_2 + H_2O = H_2CO_3 \quad (2.7)$$

$$H_2CO_3 = H^+ + HCO_3^- \quad (2.8)$$

$$HCO_3^- = H^+ + CO_3^{2-} \quad (2.9)$$

$$CaSO_4 + CO_3^{2-} = CaCO_3 + SO_4^{2-} \quad (2.10)$$

As the local pH at the cathode surface increases, *reaction 2.8* and *2.9* shifts to the right and *reaction 2.10* consequently shifts to the right forming more calcium carbonate at the steel surface, also known as calcareous deposits. $Mg(OH)_2$ can also precipitate on the steel surface and form calcareous deposits in combination with $CaCO_3$. $Mg(OH)_2$ has a lower solubility-product constant compared to $CaCO_3$, $6*10^{-10}$ and $3.8*10^{-9}$ respectively [12], and for that reason, $Mg(OH)_2$ will precipitate at a higher pH compared to $CaCO_3$. When steel is under CP

in seawater, the pH close to the steel surface becomes more alkaline as oxygen is reduced and the deposition of $CaCO_3$ is expected to occur first [12]. The deposition of the calcium carbonate reduces the transport of O_2 to the steel surface and thus reduces the rate of the cathode reaction (*reaction 2.2*). As a result, the required current demand and hence the protection current the anodes deliver is reduced. This increases the lifetime of the anodes due to the reduced required current the anodes have to deliver. The formation of calcareous deposits is considered in CP standard where the current density on the steel surface is dependent on the formation of calcareous deposits [5, 11].

2.1.4 The Reduction Reactions

During CP, the two reduction reactions that may occur is the hydrogen evolution reaction (HER) and the ORR. These two reactions occur by different mechanisms, where the HER is activation controlled and the ORR is mass transport controlled. The activation-controlled reaction is the transfer of electrons and can be described by the Tafel approximation of the Butler-Volmer Theory [13]. The ORR is controlled by transport of oxygen to the metal surface and the oxygen reduction limiting current is an important parameter in CP models because the rate of diffusion-controlled reaction is directly related to the current applied to the cathode surface by the CP system [14].

An important aspect of CP in seawater is the current requirement to the steel surface. during the initial stage of the polarization of the steel, ORR dominates due to the lack of calcareous deposits. With time, the calcareous deposits grow, and the rate of ORR decreases and the HER takes over as the reduction reaction at the steel surface [15].

Okstad et al. [15] investigated the effect of calcareous deposits on the reduction reactions. When calcareous deposits were established at the steel surface, hydrogen evolution dominated at potentials more negative than -950 to -1000 mV. Oxygen reduction was the most important reduction reaction at potentials more positive that -800 to -900 mV.

2.1.5 Current Requirement

CP standards [4,5,6,7] recommend three current density values according to the environmental region: an initial, mean and final [9]. The initial current density is high due to the lack of

calcareous deposits and since the potential difference between the anode and the steel surface is largest initially, and it is the current density required to polarize the exposed steel surface. The mean value is the current density demand once the CP system reaches a stabilized condition, and this value is used to calculate the minimum anode mass required to protect the system during the design lifetime. The final current density takes into account that the CP system has to repolarize the structure and form a new calcareous layer in an event of removal of these layers [16]. The current density values are used to calculate the total current demand, I_c, which is dependent on the cathode surface area, A_c. The Total current demand is calculated according to the following equation:

$$I_c = A_c * i_c \tag{2.7}$$

As mentioned, the coating reduces the current demand by reducing the cathode surface area and *equation 2.7* is modified to include a coating breakdown factor:

$$I_c = f_c * A_c * i_c \tag{2.8}$$

The coating breakdown factor is dependent on the lifetime of the CP system, the thickness and type of the coating. The two constants, *a* and *b*, are coating properties and *t* is the lifetime [5].

$$f_c = a + b * t \tag{2.9}$$

The total current output per anode, I_a, can be calculated using Ohm's law (*equation 2.10*) and it is acceptable for three-dimensional structures to assume that the anode-electrolyte resistance, R_a, is dominant and neglect the metallic resistance and thus consider $R_t = R_a$. With this assumption and also by assuming a constant cathode potential the current output from an anode can be expressed as [9]:

$$I_a = \frac{\phi_c - \phi_a}{R_a} \tag{2.10}$$

where ϕ_c is the closed-circuit potential of the cathode and ϕ_a is the closed-circuit potential of the anode. For one-dimensional structures, as marine pipelines, the potential drop in the metal cannot be neglected when the distance between the anodes is large and thus the metallic

resistance cannot be neglected. The metallic resistance can be expressed as a function of the cross-section area, the length of the pipeline and the resistivity of the pipeline material [9]:

$$R_m = \frac{\rho_m * L}{A} \tag{2.11}$$

For simple spherical and cylindrical shapes, anode resistance can be evaluated and calculated using classic resistance equations such as Dwight's and McCoy's equation (*equation 2.12*), where Dwight is used when the length of the anode is much longer than the anode radius and McCoy is valid for bracelet anodes [9]. R_a is the anode resistance, ρ_e is the electrolyte conductivity and S_a is the exposed anode area.

$$R_a = \frac{0.315 * \rho_e}{\sqrt{S_a}} \tag{2.12}$$

2.1.6 **Electric Field**

As there is a potential difference between the anode and the cathode, the anode can be considered as a negative charged surface and the cathode a positive charged surface. Hence, the anode supplies the cathode surface with electrons, referred to as a current. As the current flows through the electrolyte, an electric field is created. The electric field has the same direction as the electric force acting on the electrons, which is the same direction as the electron flow, illustrated in *Figure 1*.

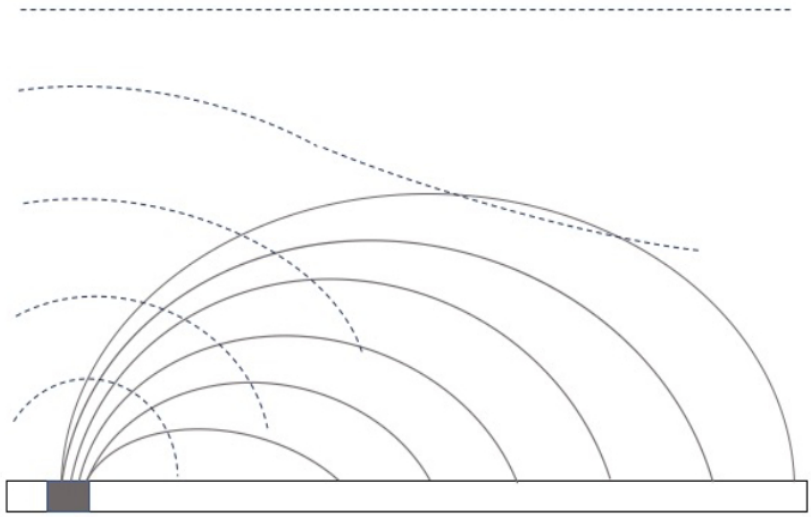

***Figure 1**, Electric field lines created between the anode and the cathode when the anode is supplying current to the cathode uniformly. Equi-potential field lines are included as dotted lines.*

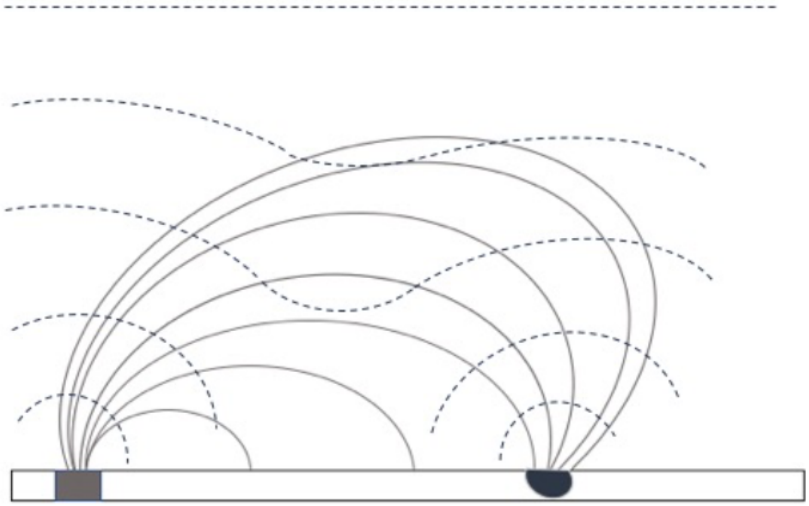

***Figure 2**, Electric field lines when the anode is supplying current to the cathode surface when a coating damage is present. Equi-potential field lines are included as dotted lines.*

Figure 2 illustrates how the electric field changes as a coating damage is present. The density of the electric field lines increases locally at the location of the coating damage since the anode is supplying more current to this area. Equi-potential field lines are included in both *Figure 1* and *Figure 2*, illustrated as dotted lines. The equi-potential field lines become flatter and more constant as the distance away from the pipe approaches the position of the remote reference electrode. The position of the reference electrode relative to the pipeline is seen in *Figure 3*.

2.2 Measurements of CP systems

2.2.1 Measurements Techniques

There are several methods available to measure and evaluate the performance of a CP system based on CP inspection by the use of remotely operated vehicle (ROV). Depending on the level and detail of information required, there are four different methods that are used for ROV based pipeline survey [18].

- Proximity half cell
- Single point contact system (Spot CP)
- Single point contact with continuous CP (Cell to Cell Method)
- Single point contact with continuous CP and field gradient

Pipeline potential measurements are performed by the use of electrode probes, which have been used for measuring the cathodic protection potential since the early eighties [17]. The Cell-to-Cell technique uses an Ag/AgCl electrode probe in combination with a remote Ag/AgCl half-cell electrode which provide a stable reference, also known as a reference electrode. The electrode probe connected to a ROV and the reference electrode are illustrated in *Figure 3* [36]. Regular contact measurements are obtained during the survey to provide potential measurements at given locations. To provide a baseline measurement, the natural potential between the electrode probe and the reference electrode are zeroed and the value at the local measurement obtained during the contact with the steel or the anode is added. Any variations in potential measured are only caused by local changes in potential as the electrode probe moves along the pipeline inspected [18].

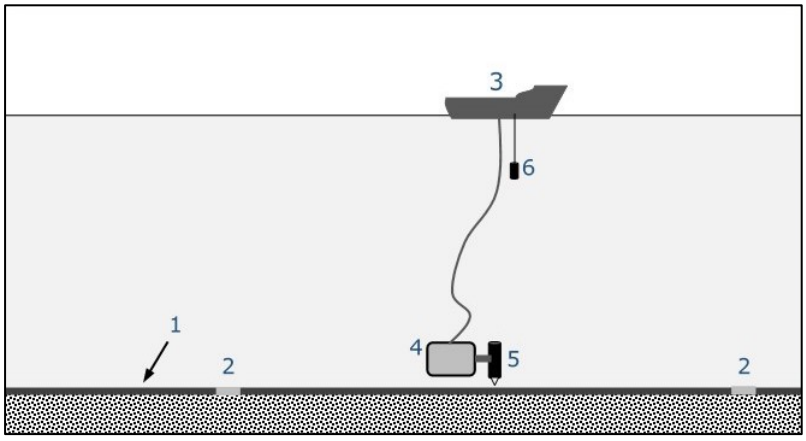

***Figure 3**, Close-To-Remote CP Pipeline Inspection. 1) subsea Pipeline, 2) Bracelet Galvanic Anodes, 3) Vessel, 4) ROV, 5) Two-Electrode Probe and 6) Remote (Reference) Electrode.*

The Twin Half-cell contact probe is similar to the one used in Cell-to-Cell method, except that another Ag/AgCl electrode is incorporated. This addition of an extra electrode in the probe body makes it possible to obtain field gradient measurements allowing anode current density and output to be calculated, and thus the remaining life of the anodes [18]. Continuous potential measurements are possible when both methods are used, and an illustration of a potential profile of a pipe with one anode and two different coating damages is illustrated in *Figure 4* [8]. As the distance of the reference electrode increases relative to the pipeline, the potential profile consequently becomes flatter and the potential differences decreases [8]. As a consequence, coating defect becomes more difficult to measure as the distance between the pipeline and the electrode probe increases.

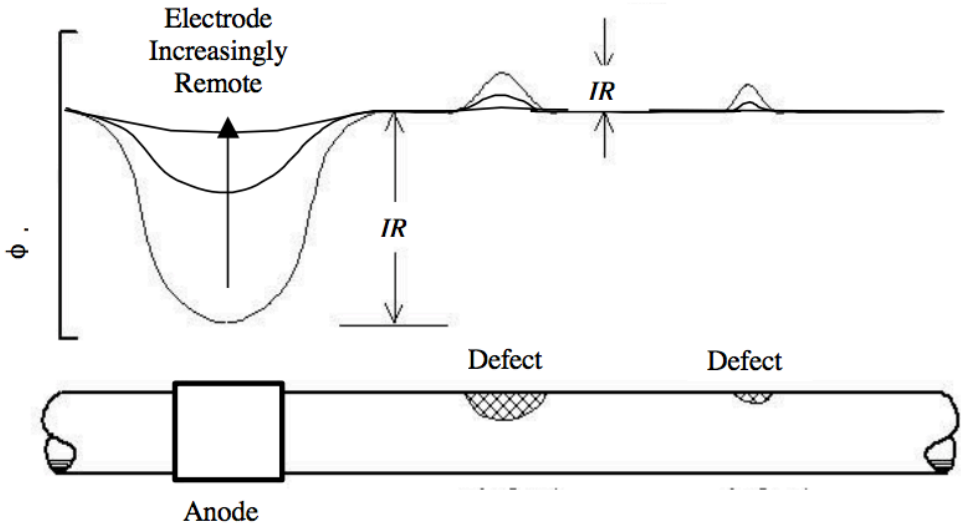

***Figure 4**, Potential profile for a pipeline recorded by an over-the-line survey.*

In 1991, Jim Britton introduced the possibility of developing a field gradient scanner that could provide multi-directional field gradient and potential information for large subsea and offshore structures, such as platforms [17]. The project was, however, not successful and was terminated in 1988. In 2014 [37], FORCE Technology introduced the field gradient sensor, FiGS®, which provides both magnitude and direction of the electric field based on a twin-cell configuration. The electric field gradient is the rate of change in the electric field, which is measured by the FiGS®, and field gradient values are equal to the difference in the potential in the two half-cells in the measuring probe divided by the distance between them. A potential profile is obtained when the sensor is moved along the pipeline and measures the electric field gradient continuously.

2.2.2 Parameters Affecting the Measurements

As mentioned in *section 2.1.2,* SA are commonly used to protect subsea pipelines and the anodes for this purpose are usually of a bracelet type. The electric field created between the anodes and the cathode is affected by several parameters such as anodes/pipeline being buried, burial depth, water depth, mud/sediment and seawater resistivity and current drain to either wells or anchor chains [2, 6].

If a pipeline is buried (fully or in sections), this affects the potential profile of the pipeline since the resistivity of the seabed sediments/mud is different from the resistivity of the seawater. The

resistivity of seabed sediments is also dependent on the geographical location. In the 80's, mapping of the seabed sediment properties was performed [19]. The resistivity ranges from 33 – 250 Ωcm at 20 °C and the recommended value in ISO 15589-2 is 130 Ωcm [7] which is higher than the resistivity in most locations at the NCS, except at 71 – 72 °N [19].

Buried pipe sections also includes the effect of rock dump, which is a difficult problem to consider because the resistivity of the rock dump is unknown. A rock dump makes sure to keep the pipeline at the intended location and prevent movement. In practise, the resistivity of a rock dump is regarded as the resistivity of sediments according to the ISO 15589-2 standard [7]. The composition of a rock dump varies with respect to rock size, sand and water content in between the rocks. In CP design, a value of 150 Ωcm [7] or 130 Ωcm [4] should be used, but realistic resistivities of a rock dump can be estimated based on void fraction of the rock dump and the resistivity of the medium filling the voids in between the rocks [20].

Current drain is a parameter that is not well described because in CP design this parameter is just considered as fixed [4, 5, 6, 7]. The ISO 15589-2 recommend including a value in the range of 1.5 A to 5 A per well in the total design current density requirements [7], while the DNV-RP-B401 recommend that a current drain of 5 A per well should be included in the current drain calculations [4].

2.2.3 Anode Monitoring

Anode monitoring is performed in the same way as the pipeline, by different types of probes and sensors. If regular stab probes are used for anode measurements, only give potential information and not current output and remaining lifetime is obtained [18]. The field gradient sensor, FiGS®, described in *section 2.2.1*, does also provide anode information as current output. All sensors or probes available for anode or pipeline measurements required either ROV or divers to do the measurements.

Another alternative to anode measurements is the use of constant monitoring, where an instrument package is designed for anode current output, potential and temperature measurements [21]. This system provides measurements without requiring survey equipment.

2.3 Mathematical Model for Corrosion Analysis

2.3.1 Computer Modelling

Computers have been used to evaluate CP systems since the late seventies [22]. The finite difference method (FDM) was the first method used in electrochemical system analysis where only simple geometries were studied. Due to the lack of stability in solving complex geometries, FDM was replaced by the finite element method (FEM). The latest method developed for modelling CP systems is the boundary element method (BEM) [22].

COMSOL Multiphysics [38], a software for computer modelling, uses both FEM and BEM because both methods have their advantages and disadvantages. When physical equations are being solved for a geometry, the geometry has to be broken up into elements, also known as discretization of the geometry. The equations are solved at certain points in each element and a finite set of equations are created due to the relationship between the elements in the geometry. The FEM only describes the relationship between neighbouring elements, so when this method is used, the volume of the entire geometry has to be discretised to create the necessary set of equations. With BEM, only the boundaries on the geometry have to be discretised, simplifying the model and making it easier and less time consuming to solve [23].

BEM has been the preferred method numerical simulation of CP systems since the early 80's due to its high computational efficiency compared to other methods such as FEM. Due to the discretization of only the surface of the structure, BEM was particularly appealing for models involving semi-infinite domains because it doesn't require to evaluate the potential and current density for the whole electrolyte volume, and it has been found particularly suitable for CP modelling in seawater [14]. Even though the BEM has several advantages, it also has important limitations. It has difficulties modelling electrolytes with non-homogenous resistivity and CP systems where the air-electrolyte interface has a complex geometry. Due to these limitations, BEM is found insufficient for modelling complex CP systems for underground and reinforce concrete structures [14].

The FEM, on the other hand, allows numerical simulations of complex geometries. This is achieved by dividing the modelled domain into elements of simple geometry. The equations are then solved for each element and the solution for the whole domain is reconstructed by

adding together the contribution of each element. The FEM can also handle heterogenous and dynamic environments because the properties of the environment can be defined independently for each element [14].

2.3.2 Modelling the Electrolyte

As a result of corrosion, a net flow of ionic species is transported through an electrolyte by several ways: migration, diffusion and convection [14]. Migration is the movement of ions due to the presence of an electric field. Diffusion occurs when there is a difference in concentration of the ionic species in the electrolyte that forces the species to move from high concentration to low concentration. When the ionic species are transported due to the transport of the electrolyte itself, the movement of the species is called convection. When CP problems are modelled using FEM, there are two commonly used equations used for describing the behaviour of the electrolyte: the Nernst–Plank and the Laplace equations [14].

The Nernst–Plank equation considers diffusion, migration and convection of the ionic species to describe the electrolyte, *equation 2.13* [24]. The electrolyte is maintained electrically neutral and the concentration of all the chemical species is balanced as a function of the different transport mechanisms. By the use of this approach, the rate of each chemical reaction can be described individually, which makes this a very detailed and accurate description of the system. As detailed approach as the Nernst-Plank also comes with some drawback. With such a level of details, it requires knowledge of the entire system as diffusion coefficients and electric charge of all the species, and reaction kinetics and constants of all the chemical reactions. With all these required parameters considered, the Nernst–Plank approach is for most practical cases limited due to the amount of iterations required to balance the concentrations of all the species combined with the amount of knowledge of the system [14].

$$-J_j(x) = D_j \frac{\partial C_j(x)}{\partial x} + \frac{z_j F}{RT} D_j C_j \frac{\partial \phi(x)}{\partial (x)} + C_j v(x) \tag{2.13}$$

where:

J(x) = unidirectional flux of species j (mol/cm^{2}s)
D_j = diffusion coefficient of species j (cm^2/s)
∂C = variation of concentration (mol/cm^3)

∂x = variation of distance (cm)

z_j = electric charge of species j

F = Faraday's number (kJ/V mol)

R = gas constant (J/K mol)

T = absolute temperature (K)

C_j = bulk concentration of species j (mol/cm^3)

$\partial \phi$ = variation of potential (V)

v = forced velocity of ion (cm/s)

A simpler description of the electrolyte can be obtained by Laplace equation (*equation 2.18*) where a potential distribution in the electrolyte surrounding a structure under CP can be obtained. This approach considers Ohm's law in three dimensions and only requires knowledge of the electrolyte's resistivity. The advantage of this approach compared to the Nernst–Plank equation is that the variables are relatively easy to be measured and it is suitable for large CP systems where the distribution of individual species is of less interest. Electrically neutral species such as gases can, despite that the approach ignores the transport of individual species, be included in the model easily [14].

The use of softwares in computer modelling solves the Laplace equation to obtain the potential distribution. The Laplace equation can be obtained from the equation for the current density of the electrolyte [25]:

$$i_j = -F \sum_{i=1}^{N} z_i D_i \frac{\partial c_i}{\partial x_j} - F^2 \sum_{i=1}^{N} z_i^2 c_i u_i \frac{\partial \phi}{\partial x_j} \quad (2.14)$$

where i_j are the components of the current density vector and F is the Faraday's constant. z_i is the charge, c_i the concentration, u_i the mechanical mobility and D_i the diffusion coefficient for species i. N is the number of species and ϕ is the electrochemical potential. The electrolyte's conductivity can be defined as [25]:

$$k = F^2 \sum_{i=1}^{N} z_i^2 c_i u_i \quad (2.15)$$

The concentration profile in the electrolyte has to be assumed uniform. The concentration gradients only influence the diffusion layer close to the cathode surface and compared to the

length and size of the system, this diffusion layer is very thin. The concentration gradients can for this reason be neglected in large systems which is represented in the first term in *equation 2.14*. The current density equation in the electrolyte then becomes [25]:

$$i_j = -k\frac{\partial \phi}{\partial x_j} \tag{2.16}$$

Conservation of charge requires that the derivative of the current density with respect to x equals zero [25]:

$$\frac{\partial i_j}{\partial x_j} = \frac{\partial}{\partial x_j}\left(-k\frac{\partial \phi}{\partial x_j}\right) = 0 \tag{2.17}$$

The conductivity can be assumed constant and thus, equation 2.17 reduces to the Laplace equation for the electrochemical potential ϕ [25]:

$$k\nabla^2\phi = 0 \tag{2.18}$$

FEM reduces the Laplace equation for the electrolyte to a surface equation by the application of Green's theorem [26], which transforms the Laplace equation into a linear system of equations [27]:

$$GQ = H\phi \tag{2.19}$$

where G and H are the matrices of influence coefficients of the geometry of the system, and Q and ϕ are the vectors of potential gradients and potential on the boundaries of the system. A detailed derivation of *equation 2.19* is shown in the Appendix A [28].

2.3.3 **Modelling the Electrodes**

One of the challenges in modelling CP systems is the electrode/electrolyte interphase. In most cases, this interface is described by classic electrochemical models such as the Butler-Volmer equation, where the parameters used are extrapolated from polarization curves obtained in controlled conditions [14]. The Butler-Volmer equation is based on the anodic and cathodic

reactions taking place on each electrode and hence the anodic and cathodic current density. The sum of these current densities is what is known as the Butler-Volmer equation [29], *equation 2.20*:

$$i_{net} = i_{anodic} + i_{cathodic}$$
$$= i_o \exp\left((1-\alpha)\frac{zF(\phi-\phi_0)}{RT}\right) - i_o \exp\left(-\alpha\frac{zF(\phi-\phi_0)}{RT}\right) \quad (2.20)$$

Some limiting cases of the Butler-Volmer theory can be derived, and these cases are dependent on the amount of overpotential ($\eta = \phi - \phi_o$) and the transfer coefficient (α). For small overpotentials, $|\eta| << \frac{RT}{zF}$, the Butler- Volmer equation can be linearized leading to a linear relation between current density and overpotential:

$$i \sim i_o \frac{zF\eta}{RT} \quad (2.21)$$

When the overpotential is large, $|\eta| >> \frac{RT}{zF}$, the Butler-Volmer equation can be simplified to the Tafel equation that predicts an asymptotic linear dependence where the slope is related to the transfer coefficient [29].

$$i \sim \begin{cases} i_o \exp\left((1-\alpha)\frac{zF\eta}{RT}\right), \eta \gg \frac{RT}{zF} \\ -i_o \exp\left(-\alpha\frac{zF\eta}{RT}\right), \eta \ll -\frac{RT}{zF} \end{cases} \quad (2.22)$$

The relation between the current density and the overpotential can be illustrated in a Tafel plot where η has a slope equal $(1-\alpha)\frac{RT}{zF}$ for the anodic current and $\alpha\frac{RT}{zF}$ for the cathodic current [29].

There are also two limiting cases related to the transfer coefficient. One is when the electron transfer is symmetric (α = ½) and the second is when the electron transfer is asymmetric (α = 0, 1). In both cases, the Butler-Volmer equation can be express in another mathematical form. When α = ½, the overpotential and the current density can be expressed as a hyperbolic sine dependence, *equation 2.23* [29].

$$i = 2i_o \sinh\frac{zF\eta}{2RT} \tag{2.23}$$

Figure 5 [29] shows the effect of different values of α with respect to η and i.

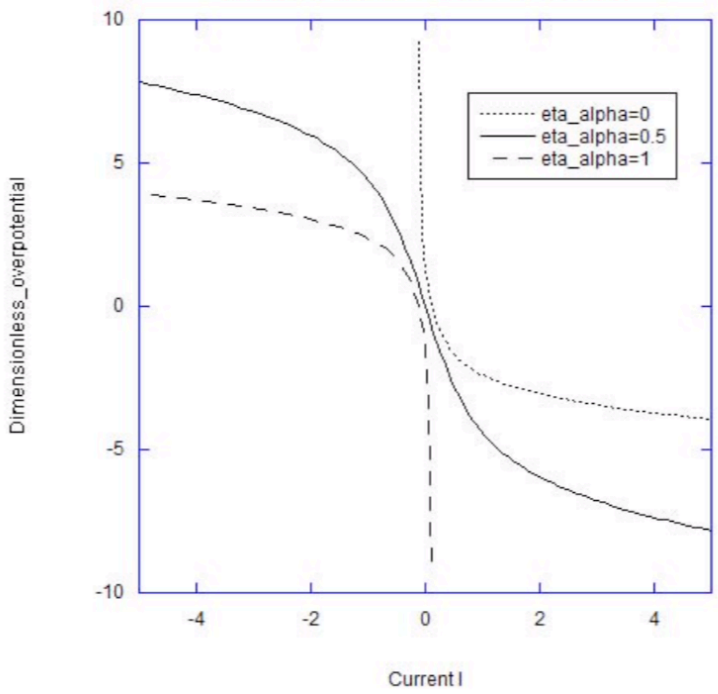

***Figure 5**, The relation between current density and overpotential for symmetric and asymmetric electron transfer coefficient.*

To solve these different equations describing the relation between overpotential and current density on electrode surfaces, boundary conditions (BC) are necessary. The BC are different for the anode and the cathode, since the cathode surface will polarize, and the polarization of the anode surface can be assumed insignificant. On the anode, the BC can either be defines as a constant current value [30], which is the Neumann boundary condition:

$$\frac{\partial\phi_{x,y,z}}{\partial n_{x,y,z}} = -\frac{i_0}{\sigma} \tag{2.24}$$

or the BC can be defined as a constant potential value [30], called the Dirichlet boundary condition:

$$\phi_{x,y,z} = \phi_A \tag{2.25}$$

where $\phi_{x,y,z}$ represents the potential of the coordinate x, y and z, and $n_{x,y,z}$ represents the direction of this coordinate, i.e. the normal to the boundary [30,31].

The cathode boundary condition can be defined by a polarization curve, which express the relation between the potential and the current density or the Butler-Vomer equation [30, 32]:

$$\frac{\partial \phi_{x,y,z}}{\partial n_{x,y,z}} = -\frac{f_c}{\sigma} \tag{2.26}$$

where f_c is the polarization function on the cathode surface. The Butler-Volmer method describes the interface between the electrode and the electrolyte in terms of a constant polarization curve, but in reality, the surface of the electrode is affected by factors as formation of passive films, accumulation of corrosion product or calcareous deposits. To include these aspects in a model, dynamic boundary condition that consider calcareous deposits on the cathode surface has to be used [14].

3 Literature Review

Computer modelling of CP problems has been a topic of great interest in the field of research the last decades, but there is a limited amount of studies regarding current drain to subsea wells. CP design standards [4,5,6,7] have their recommendations regarding drain and current densities on the cathodic surface, but evaluations of these recommendations are not something that is well studied. However, the literature review is focused on differed aspects that is important in a numerical model, as the importance of the environment surrounding the anode and cathode, and boundary conditions.

One of the most important boundary conditions regarding CP is the relation between current and potential on the electrode surfaces. One of the most known relations is the Butler -Volmer equation, which describes the relationship between current and potential when there are no limitations regarding mass transport. Li et al. [31] studied the use of a dynamic cathodic boundary conditions based on Ohm's law instead of using a polarization curve or the Butler-Volmer equation. The dynamic boundary condition considered the apparent surface resistance (R_p) which is affected by the cathodic surface conditions and contains two parts: the electrochemical reaction resistance (R_{ct}) and the film resistance (R_f) of calcareous deposits which is dependent on the thickness and the porosity of the deposits. The R_p values describe the formation of calcareous deposits with time, and the values of the surface resistivity was fixed different values at different polarization times. They found good agreement comparing the results from the numerical modelling with experimental results, which means that the use of the dynamic boundary condition was suitable to create accurate results based on numerical modelling.

Recently, Min et al [32] established a mathematical model of cathodic protection to provide guidance for the determination of cathodic protection parameters and evaluating the well casing through non-uniformity environment containing sea water, sediments and rock. They compared the potential along a well casing surrounded by all the three mentions environments, with a layer of seawater at the top, sediments in the middle and a thick layer of rock at the bottom. Experiments were also performed, where the potential profile along the well casing where measured. The conductivity of the seawater, sea mud and rock were 4.12 S/m, 1.91 S/m and 0.11 S/m respectively. The model based on FEM were compared to the measured potential profile in the experiment, and the results showed that due to different conductivities in the

environment, sudden changes in the potential along the well was observed. In addition, the potential decreased rapidly in the rock zone and only a third of the pipe emerged in rocks had a protection potential more negative that -0.8 V [7]. The results from the modelling were in good agreement with the experimental results. This result shows the importance of knowing the conductivity of the environment in a CP system, especially if a low conducting medium as a layer of rock is present.

Wigen et al. [33] investigated the drain to buried structures such as piles. They stated that the drain to mud exposed steel is according to NACE SP0176 [39] 1.5 A to 5 A per pile, while according to DnV RP-B401[4] is 20 mA/m^2 for the total surface area below the mud line. The recommended CP design from both standards were investigated and the results differed by almost 50%. Based on DnV RP-B401[4], the total drain to mud exposed steel was 181 A. Based on NACE SP0176 [39] the same drain was in the range of 67.56 A to 96.56 A, depending on if 1.5 or 5 A per pile was chosen as design criteria. Anyway, the results show that the current drain to mud exposed steel is very dependent on which design standard that is chosen. This paper shows that there is need for more knowledge regarding buried structures, and subsea wells fall under this category.

When it comes to current drain to wells, only one study has been found in the literature. Gartland and Bjørnaas [34] investigated the current drain from subsea CP systems to wells in the North Sea for two different field, the Njord and the Visund field. They compared simulated current drain to calculated current drain in accordance to the CP design. The simulated current drain was a time simulation according to the design life, which was 16 years at Njord and 30 years at Visund. The study comprises the effect of different parameters such as interference between wells and soil resistivity. The study also investigated the dependence of well depth and casing geometry on the current drain. The results from the current drain show that during the first years of the lifetime, the current drain agrees well with the CP standard used in the modelling, but with time the current drain is reduced and differ from the recommended value in the CP standard. According to the results, a current drain of 3 A and 6.7 A respectively for Njord and Visund could be used instead of 8 A recommended by the NORSOK M-503 [6]. As a consequence of the results, a reduction in the number of anodes that have to be installed is suggested due to the decrease in current drain over time.

There are different aspects of a numerical simulation that is difficult to assess, where rock dumped anodes are one of them. The resistivity of a rock dump is according to CP standards [4, 7] assumed equal to seabed sediments. Lauvstad et al. [20] investigated the effect of different rock dump characteristics, where different rock sizes, soils and porosities were used to assess more accurate values for the resistivity of a rock dump. Based on Archie's law, the resistivity of a rock dump can range from 120 Ωcm to 1000 Ωcm, depending on the porosity. Compared to the resistivity of sediments of 150 Ωcm, assuming equal properties for a rock dump as for sediments, a large error in modelled results compared to real data can be a consequence.

The geometrical parameters of the well casing, as the casing radius and the well depth, are information that is often not provided. Information of the depth of a well, if the oil and gas field is on the Norwegian continental shelf, can be found at the homepage of the Norwegian petroleum directorate [35]. This information gives an indication and a good approximation of the value that can be used as the depth of a well during computer modelling. The radius of a well casing is more described in published literature where computer modelling, or CP design are investigated. The value of the radius is often dependent on the depth of the well. Gartland and Bjørnaas [34] used a radius of 0.381 m at the top and 0.089 m at the bottom in their model simulating current drain to subsea wells. Zhang et al. [30] used a radius of 0.254 m at the top and 0.089 at the bottom modelling cathodic protection of deep well casings. Bazzoni and Briglia [40] published an article regarding CP design of gas well casings where information of the well casings was provided. The radius at the top was 0.236 m and 0.089 m at the bottom.

4 Numerical Modelling

The modelling work in this Master Thesis is based on data from a FiGS® survey where anode current outputs are calculated based on measured electric field gradients and current drain profiles are hence created. The calculated current drain profiles are used as reference profiles during the modelling. The FiGS® survey data were measured on a field in the North Sea and is referred to as Field A. The part of Field A that is used as reference in this report contains three pipelines, two template structures and two drain points. The number of wells in each drain point is unknown and for simplicity, the number of wells in the simulations are set to be one. This simplification was also used by Gartland and Bjørnaas [34], who investigated the effect of interference between two wells. The effect was so small that they used a single well model for their simulations. *Figure 6* shows an overview of the field.

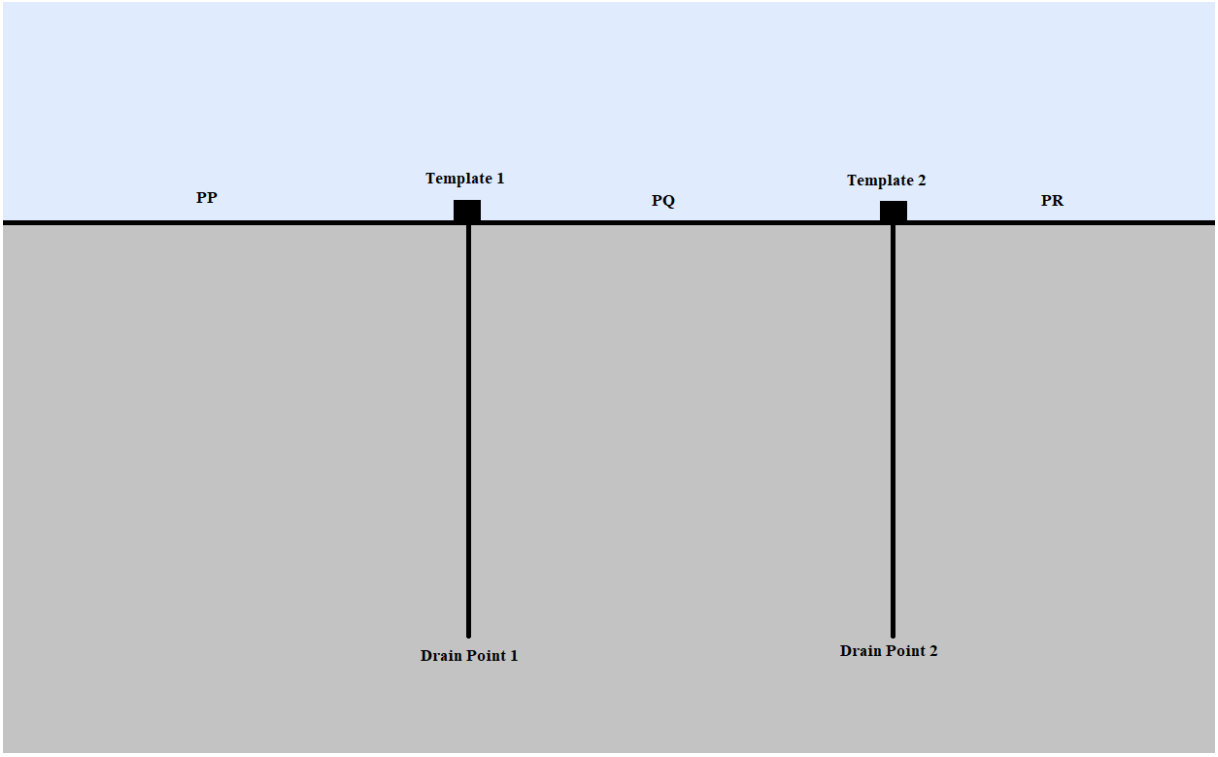

***Figure 6**, Overview of Field A, including pipes, drain points, i.e. wells, and templates. The pipelines are PP, PQ and PR.*

The pipelines, which are referred to as pipeline PP, PQ and PR, are connected to a template structure and well casings (the drain point). *Figure 7* through *Figure 9* show the reference drain profiles for the pipelines calculated from the FiGS® survey data. The number of anodes included in the models for each pipeline has to be evaluated, since not all installed anodes on the different pipelines contribute to drain to the connected drain point. From pipeline PP (*Figure 7*), the anodes from KP 0 to KP 15 are considered contributing to drain to Drain Point 1.

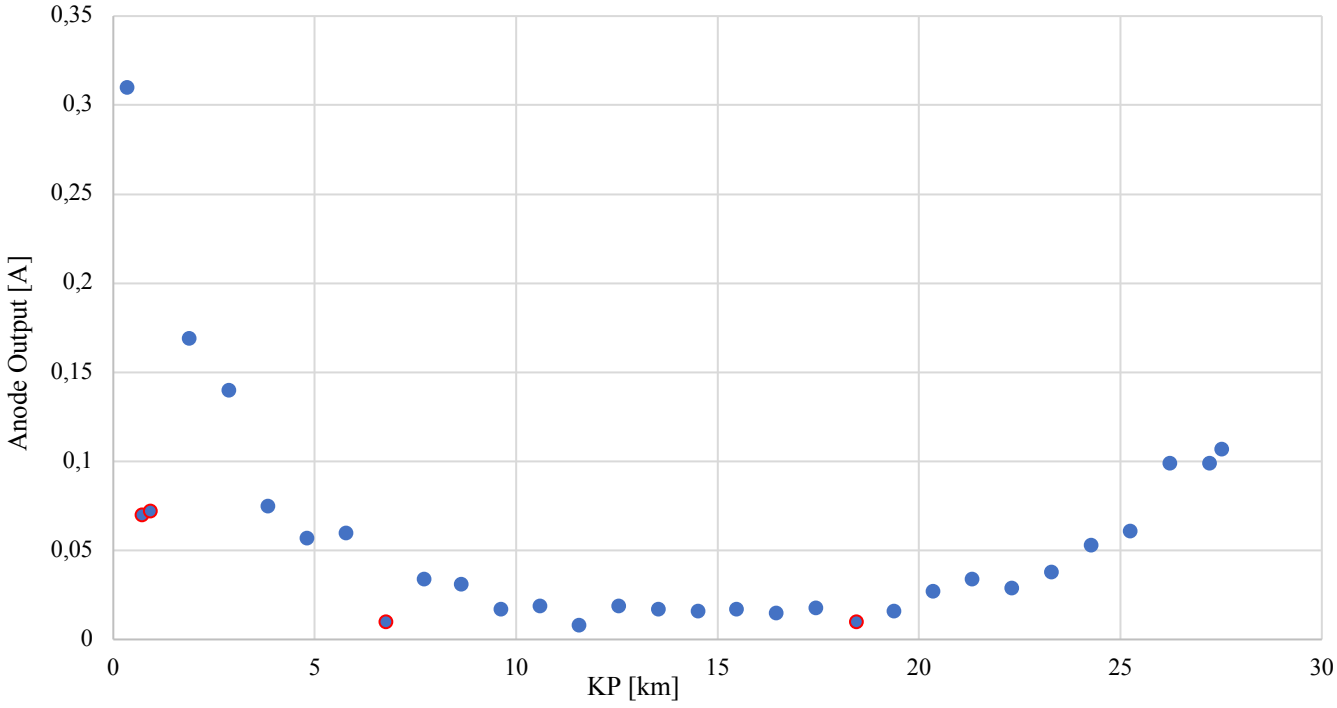

***Figure** 7, Reference drain profile of pipeline PP. Drain point 1 is located at KP 0. Red circle indicates buried anode.*

Pipeline PQ (*Figure 8*) is connected to both Drain Point 1 and Drain Point 2 and pipeline PQ is hence separated into two drain profile, one drain profile towards Drain Point 1 and one drain profile towards Drain Point 2. Based on simulations, where different set of anodes contribute to drain to the different drain points, are investigated where the set of anodes that match the reference profile the best is assumed to supply current to the different drain points. Based on the simulations, the anodes from KP 0 to KP 6 (*Figure 8*) supply current to Drain Point 2, and the anodes from KP 6 (*Figure 8*) supply current to Drain Point 1.

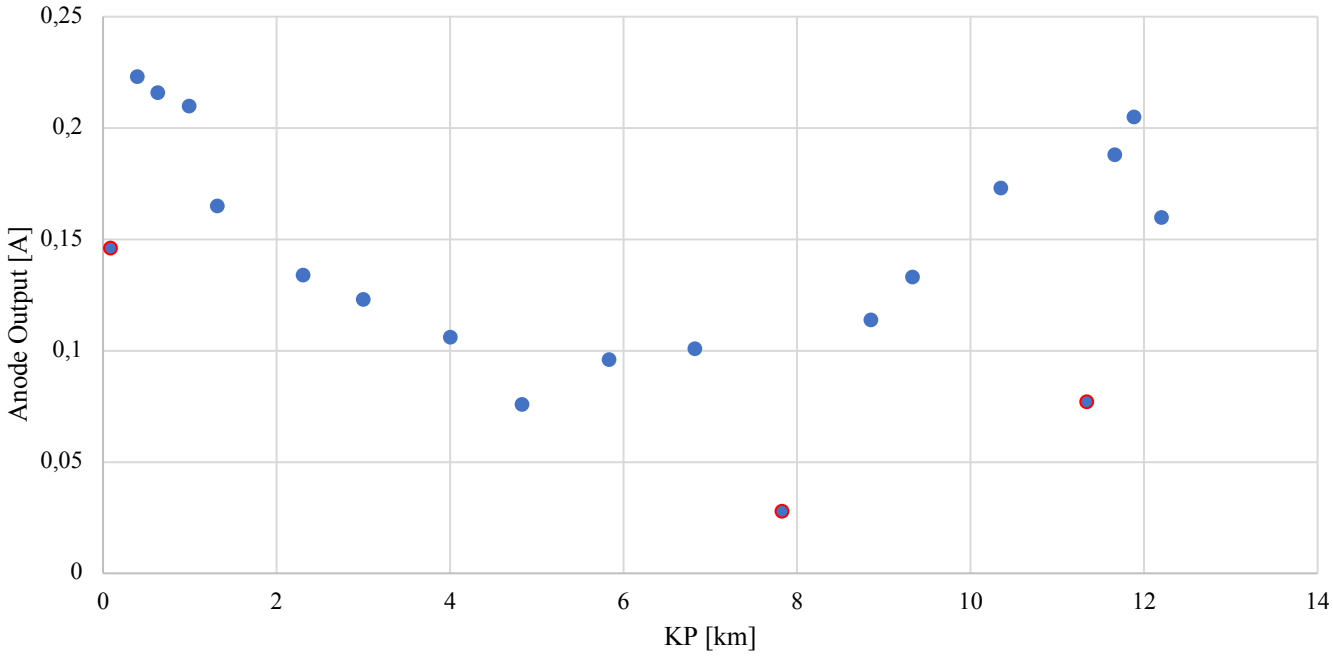

***Figure 8**, Reference drain profile of pipeline PQ. Drain Point 1 is located at KP 12.214 and Drain Point 2 is located at KP 0. Red circle indicates buried anode.*

The anodes from KP 6 on pipeline PR (*Figure 9*) are assumed supplying current to Drain Point 2, because the anode at KP 6.85 is the anode with the lowest current output. The number of anodes, their location on the pipeline and the spacing between the anodes are summarized in *Table 3* and *Table 4* in *section 4.3.2.*

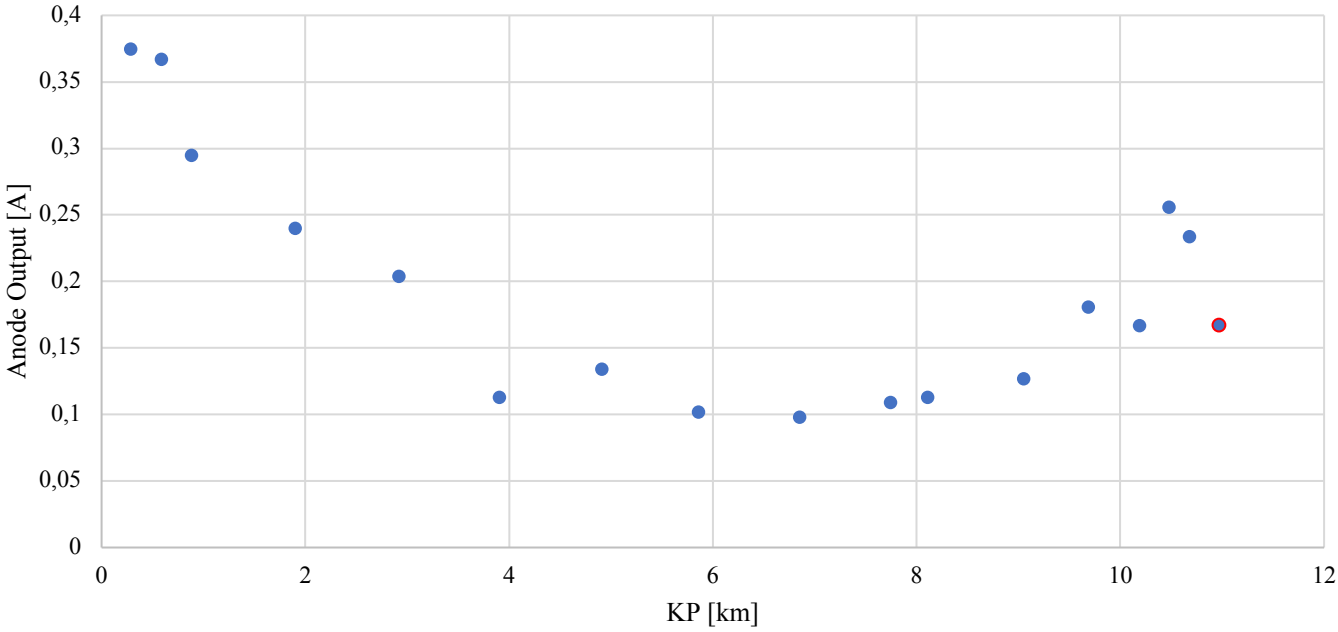

***Figure 9**, Reference drain profile of pipeline PR. Drain Point 2 is located at KP 11.136. Red circle indicates buried anode.*

Table 1 shows an overview of the amount of current drained from the different pipelines and templates to Drain Point 1 (DP1) and Drain Point 2 (DP2). The amount of current supplied to drain from the pipelines is the sum of the current output from the anodes included on each pipeline in the models minus the total amount of current supplied to the pipeline surface. The current drained from the templates is according to the survey report. The amount of current supplied to the pipeline surface is calculated based on the surface area of the pipeline sections (according to parameters in *Table 2*) and the current density on the pipeline surface according to the survey report (0.02 mA/m^2).

***Table 1**, Current drained from templates and pipelines.*

Parameter	Value	Description
$I_{PP,1}$	0.747 A	Current drained from pipe PP to DP1
$I_{PQ,1}$	1.041 A	Current drained from pipe PQ to DP1
$I_{PQ,2}$	1.339 A	Current drained from pipe PQ to DP2
$I_{PR,2}$	1.339 A	Current drained from pipe PR to DP2
I_{T1}	16.0 A	Current drained from template 1 to DP1
I_{T2}	18.0 A	Current drained from template 2 to DP2

4.1 Modelling Software

Comsol Multiphysics version 5.4 is the modelling software used in this study. The numerical technique chosen to solve the equations is the FEM. The set of equations chosen to solve the problem is defined as secondary current distribution, which accounts for the transport of charged ions in an electrolyte of uniform composition, current conduction in electrodes using Ohm's law (*equation 2.10*) in combination with a charge balance and activation overpotentials. As the concentration of individual species is neglected, the secondary current distribution uses the Laplace equation (*equation 2.18*) describing the electrolyte and not the Nernst-Planck equation (*equation 2.13*).

4.2 Modelling Procedure

Four different models are investigated in order to build a final model that matches the reference current drain profile to both Drain Point 1 and Drain Point 2:

Model 1: Drain Point 1 with drain from pipe PP
Model 2: Drain Point 1 with drain from pipe PQ
Model 3: Drain Point 1 with drain from pipe PP and pipe PQ
Model 4: Drain Point 2 with drain from pipe PQ and pipe PR

The purpose of Model 1 is to investigate the geometrical well parameters, as outer diameter, number of wells in the drain point and the depth of the wells. The slope of the cathodic polarization curve is also investigated. The effect of these parameters is investigated because the value of these parameters is unknown. To what extent they affect the current drain profile of the pipelines is important to make good assumptions for the parameters defining the well geometry in the later models. After the effect of the parameters was investigated, the geometrical parameters were fixed (summarized in *Table 2*) and Model 1 was used to find a cathodic polarization slope to obtain as good match as possible between the simulated drain profile and the reference drain profile, and this slope was used in the cathodic polarization curve in the other models.

In Model 2, drain to the same drain point is considered, but from anodes on pipeline PQ instead, to see if the model, with the same parameters, is able to match the measured drain profile for this case.

Model 3 is an expanded model, combining Model 1 and Model 2, including the entire drain to Drain Point 1 from both pipelines PP and PQ. Both pipelines have to be included because the total amount of current possible to drain by the cathodic surface is limited by the cross-section area of the well casings and the resistivity of the well casing material. The limitation regarding how much current a well can drain from adjacent CP systems, is that all the return current going back to the anodes have to flow through the wells. When several CP systems are connected to a common drain point, the return current to each CP system have to share the return path through the wells, which will limit the amount of current that can be drained by the well surface. In Model 1 and Model 2, only one CP system is connected to the drain point, and all the return

current going back to the CP system flows through the well casings and back to the pipeline's anodes. When two CP systems are connected to the same drain point, the current drained from each CP system has to share the return path through the casing cross-section. Since the amount of current possible to drain is limited by the cross-section and the resistivity of the well casing, less current will be possible to drain from each CP system. To obtain as realistic results as possible, both incoming pipelines to a drain point must be considered and the current drained from the template structure also has to be included, and the resistivity of the well casing has to be corrected accordingly.

The template structure is not included in the models, but the current drained from its anodes is considered by changing the resistivity in the well casings. It is assumed that the driving voltage between the anode and cathode surface (ΔV) is constant and independent on the amount of current drained to the well casing. According to Ohm's law (*equation 2.10*), when the driving voltage is constant and the current changes, the resistance between the anode and the cathode surface has to change. The resistance and the resistivity in the well casing is described by *equation 2.11*. The resistance is dependent on the resistivity in the well casing material, the length of the cathode and the cross-section area. As the length of the cathode (depth of the well casing) and the cross-section area are constant, changes in the well casing resistivity changes the resistance between the anode and the cathode surface. *Equation 4.1* is Ohm's law for Model 1, and *equation 4.2* is Ohm's law for Model 3:

$$\Delta V = I_1 R_1 \tag{4.1}$$

where $I_1 = I_{T1} + I_{PP,1}$, and R_1 is the resistance between Drain Point 1 and the anodes on pipeline PP.

$$\Delta V = I_3 R_3 \tag{4.2}$$

where $I_3 = I_{T1} + I_{PP,1} + I_{PQ,1}$, and R_3 is the resistance between Drain Point 1 and the anodes on pipeline PP and PQ.

Since the driving voltage is assumed the same, the resistance used in Model 3 can be rewritten by combining *equation 4.1* and *equation 4.2*:

$$R_3 = R_1 \frac{I_{T1}+I_1}{I_{T1}+I_1+I_2} \quad (4.3)$$

The accuracy and the degree of realistic results from the third model is investigated by using the same model on Drain Point 2 with drain from pipeline PQ and PR (Model 4). This model is used to verify Model 3.

4.3 The Model Geometry

The models contain an electrolyte box, including both seawater and sediment, pipeline, well and anodes. There are several rock dumped anodes, and the rock dumps are modelled as a box with a different resistivity. The parameters used in the four models are listed in *Table 2*.

***Table 2**, Geometrical Parameters used in the models.*

Parameter	Value	Description
OD_P	0.4 m	Outer diameter pipe
OD_A	0.4 m	Outer diameter anode
L_A	0.34 m	Length of anode
L_{PP}	15000 m	Length of Pipe PP towards drain point 1
$L_{PQ,\,1}$	5500 m	Length of Pipe PQ towards drain point 1
$L_{PQ,\,2}$	6200 m	Length of Pipe PQ towards drain point 2
L_{PR}	4500 m	Length of Pipe PR towards drain point 2
L_W	3500 m	Depth of the wells
OD_W	0.4 m	Outer diameter well casing
t_W	0.02 m	Well casing thickness
t_P	0.013 m	Pipe thickness
σ_s	5e6 S/m	Conductivity carbon steel
σ_w	3.33 S/m	Conductivity sea water
σ_m	0.76 S/m	Conductivity sediment (mud)
σ_{rd}	0.2 S/m	Conductivity rock dump

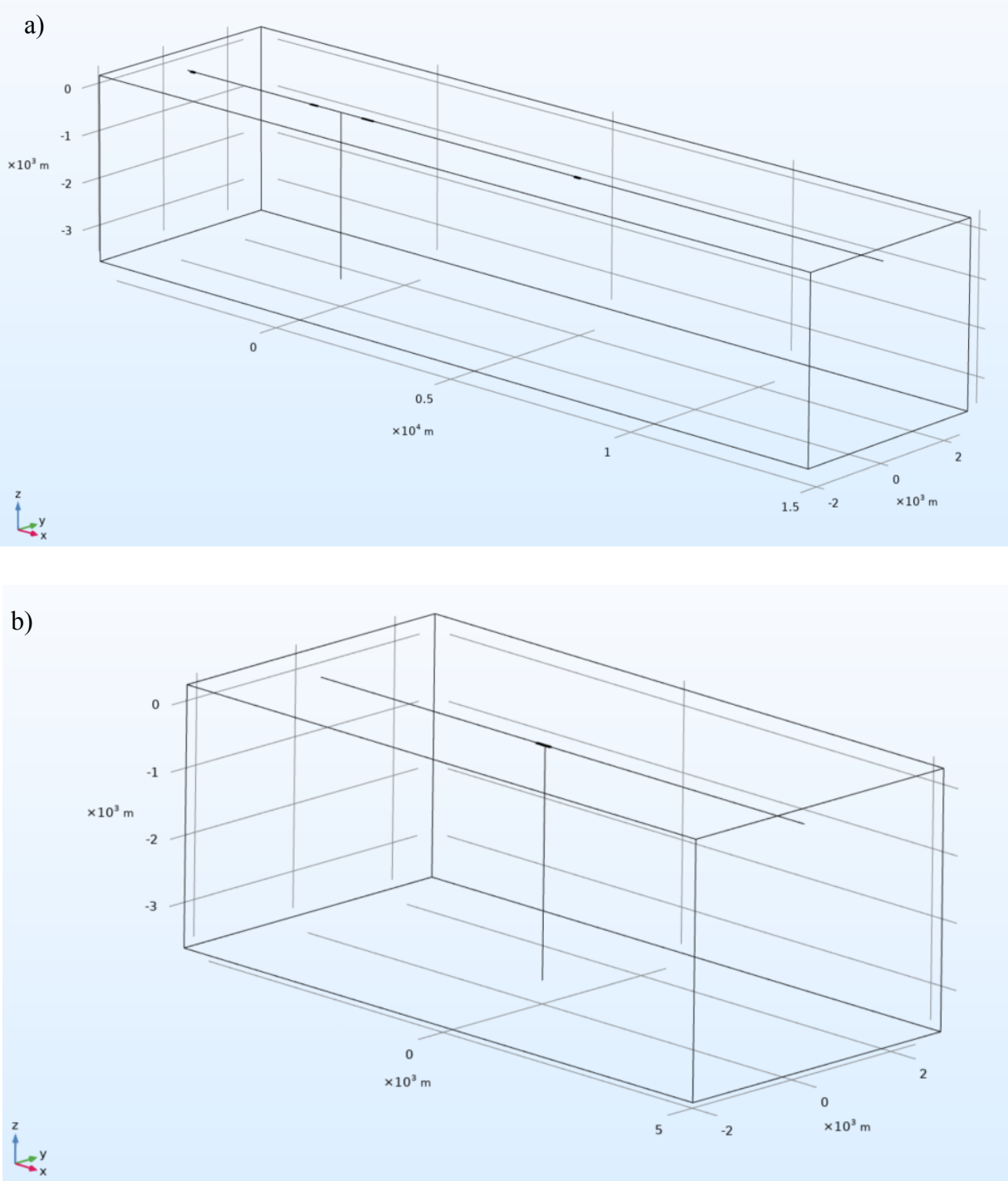

***Figure 10**, a) The geometry of Model 3 with pipe PP and PQ and Drain Point 1. b) The geometry of Model 4 with pipe PQ and PR and drain Point 2.*

4.3.1 **The Pipelines**

The pipelines are modelled as an edge element with a given radius. The pipelines have in reality a thick thermal insulation coating and due to the good coating, the current delivered to the pipe

surface is limited (0.02 mA/m^2). The current density on the pipe surface is hence set to be zero which makes it easier to evaluate the current drain from each anode to the well surface, since only drain to the well surface will be present in the simulations. Another benefit of not having a current density on the pipe surface is that it simplifies the meshing of the model. Since the pipeline is not of interest, a very coarse mesh can be applied. The pipeline is included in the model because it results in a resistance between the anodes and the drain point, which is one of the major factors determining the amount of anode current supplied to drain.

4.3.2 The Anodes

The anodes are modelled as an edge element with a given radius. The anode spacing is, according to the CP design, 300 m the first 1000 m adjacent to a template and the rest of the pipeline has an anode spacing of 1000 m. *Table 3* and *Table 4* show an overview of the number of anodes included in the different pipe sections that contribute to drain to Drain Point 1 and Drain Point 2 respectively. In the tables, both the position of the anodes and the anode spacing is included. The position of an anode is the distance away from the drain point along the pipeline. As seen in the table, the anode spacing slightly deviate from the CP design for pipeline PP, while there are larger deviations for the other pipe sections, but the shorter anode spacing the first 1000 m can be confirmed for all the pipelines.

***Table 3**, Positions of the anodes on the pipelines connected to Drain Point 1 and the spacing between the anodes.*

Drain Point 1			
Pipe PP		**Pipe PQ**	
KP [km]	**Spacing to previous anode [m]**	**KP [km]**	**Spacing to previous anode [m]**
0,348	-	0,009	-
0,714*	366	0,329	320
0,913*	199	0,548	219
1,893	980	0,875*	327
2,878	985	1,867	992
3,846	968	2,883	1016
4,816	970	3,359	476
5,785	969	4,39*	1031
6,76*	975	5,392	1002
7,727	967		
8,644	917		
9,623	979		
10,604	981		
11,57	966		
12,552	982		
13,536	984		
14,515	979		

* Rock dumped anodes

***Table 4**, Positions of the anodes on the pipelines connected to Drain Point 2 and the spacing between the anodes.*

Drain Point 2			
Pipe PQ		**Pipe PR**	
KP [km]	**Spacing to previous anode [m]**	**KP [km]**	**Spacing to previous anode [m]**
0,084*	-	0,167*	-
0,393	309	0,462	295
0,629	236	0,661	199
0,994	365	0,95	289
1,32	326	1,452	502
2,31	990	2,09	638
2,999	689	3,031	941
4,003	1004	3,396	365
4,831	828	4,286	890
5,834	1003		

* Rock dumped anodes

4.3.3 The Drain Points (well casings)

According to the homepage of the Norwegian petroleum directorate [35], the depth of the wells at Field A is approximately 3500 m, which is used as well depth in Model 2, 3 and 4. The radius of the well casings and the number of wells at each location are not known, and the effect of these parameters are hence investigated on the drain profile (Model 1). The radius of the well casing used in Model 2, 3 and 4 is 0.2 m. For simplicity, the radius is constant with the casing depth. This value is only an assumption due to the lack of information, but it is within the values found in the literature. The well is modelled as an edge element with a given radius, same as for the anodes and the pipelines.

4.3.4 The Electrolyte

The electrolyte is a box as shown in *Figure 10*. The position of the pipeline is at height (z-direction) equal zero, which means that for positive z-values, the electrolyte is seawater and for negative the electrolyte is sediment. This means that the pipeline and the anodes are assumed half buried. The height of the box is 3870 m, which is the depth of the well and the depth of the

water [35]. The width has to be large enough to not affect the current flow in the electrolyte and hence the results, and a width equal 5000 m is used in the simulations.

4.3.5 Rock dumps

There are several anodes that are rock dumped. The conductivity of the rock dump given in *Table 2* is found from simulations of Model 1, where the conductivity is one of the parameters investigated. An iteration process where several values are tested and the one that matched the anode current output of the rock dumped anodes in combination with the other parameters best was used in the other models, i.e. Model 2, 3 and 4. According to the study of rock dumps performed by Lauvstad et al. [20], the value used in the modelling is in the range of expected values estimated in the study.

The geometry of the rock dump is only a box with length equal the real length measured during the survey of Field A. According to data from the survey, the anodes that are rock dumped have a depth of burial equal 1 m. The width of the box is 40 m, but this is only an assumption due to lack of information.

4.4 Boundary Conditions

The boundary conditions used in the models are summarized in *Table 5*. The anode potential and steel potential are according to the ISO 15589-2 standard [7]. The polarization curve on the well casings is assumed to be a linear relation between current density and potential. A symmetry factor *f* is included in the cathodic polarization curve to account for drain from both the connected pipelines to the drain point when Models 1 and 2 (one pipeline only) are expanded to Models 3 and 4. If *f* equals two, it can be assumed that the wells drain an equal amount of current from both pipeline CP systems, otherwise more current is drained from one of the pipelines. *Table 6* show calculated symmetry factors used in the different models based on anode current outputs (*Table 1*) from the survey report of Field A. The slope of the cathodic polarization curve is estimated during an iteration process by simulations using Model 1, and is estimated to be 0.00065 $(A/m^2)/V$. The cathodic polarization curve (i_C) used in the other models (Model 2, 3 and 4), since it is assumed linear, is the product of the cathodic polarization slope, the symmetry factor *f* and the overpotential η.

***Table 5**, Anodic and Cathodic Boundary Conditions.*

Parameter	Value	Description
E_S	-0.6 V	Open Circuit Potential Steel (vs. Ag/AgCl)
E_A	-1.05 V	Open Circuit Potential Anode (vs. Ag/AgCl)
i_A	100*η	Polarization Curve Anode
i_C	f*0.00065*η	Polarization Curve Cathode, i.e. well surface

***Table 6**, Symmetry Factors Calculated for Model 1 - Model 4.*

	Symmetry Factor, f
Model 1	1
Model 2	1
Model 3	2.39
Model 4	2.00

The potential of buried anodes is -1000 mV vs Ag/AgCl according to the ISO 15589-2 standard [7]. If -1000 mV vs Ag/AgCl is assumed for the buried anodes in the models, these anodes become cathodic in the simulations with a negative current output. *Figure 11* shows the potential profile of Model 1 where the anode potential is investigated. As seen in the figure, when the buried anodes have a potential equal -1000 mV vs Ag/AgCl, they get depolarized to potentials more positive that the pipe surface, which means that they become cathodic relative to the other anodes. No cathodic anodes are, however, seen in the survey results. The buried anodes are, hence, assumed to have an open circuit potential of -1050 mV vs Ag/AgCl, equal to the seawater exposed anodes.

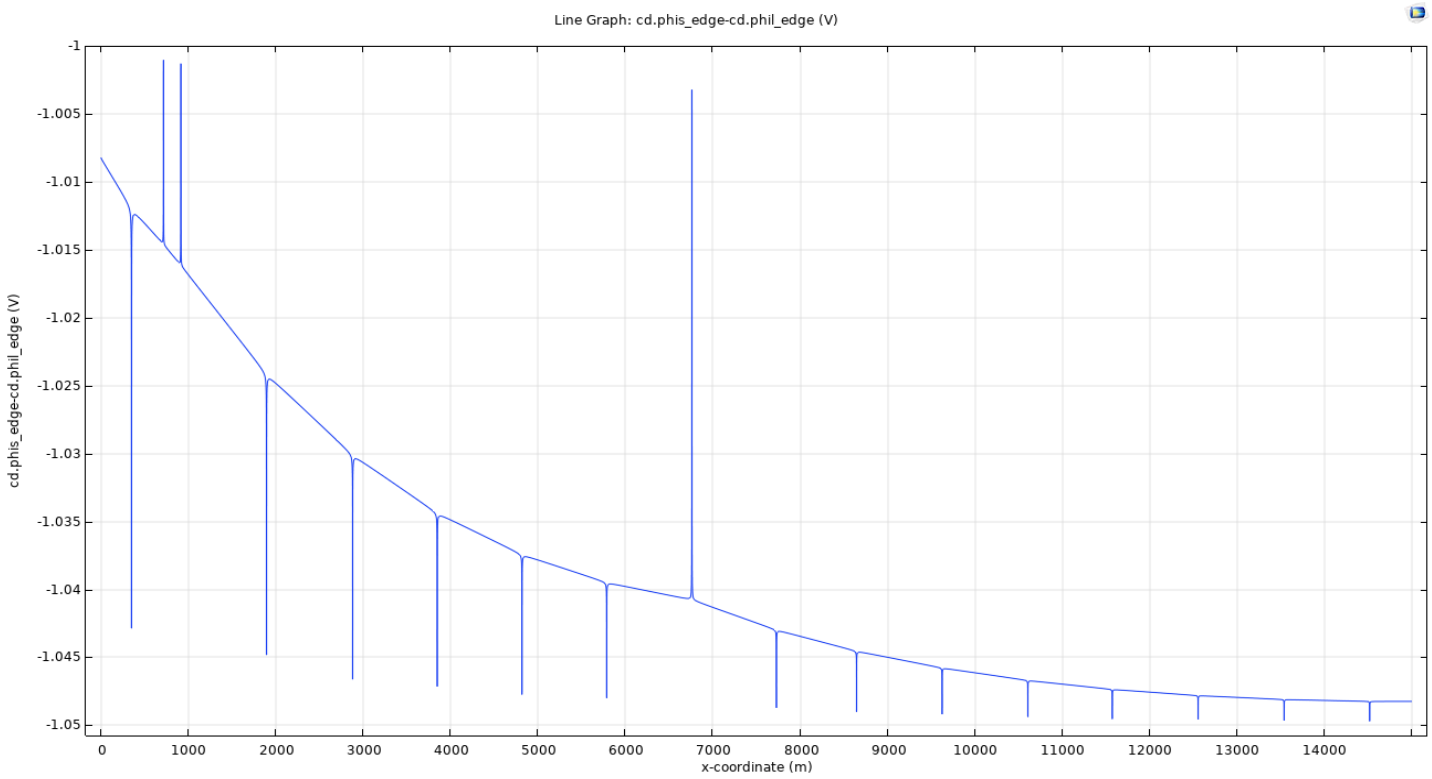

***Figure 11**, Potential profile of Model 1, with a potential equal to -1000 mV vs Ag/AgCl for the buried anodes.*

According to Deepwater Corrosion Service [41], who produces bracelet anodes designed for offshore pipelines, the open circuit potential of an aluminum-based anode is -1080 mV vs Ag/AgCl, while the closed circuit potential is -1050 mV vs Ag/AgCl. The open circuit potential is the potential on the anode when it is not connected to a cathode and no current flows through it, which means that the anode and cathode reactions are balanced. The closed circuit potential is the potential when the anode is connected to a cathode and a potential difference is present. The closed circuit potential is the potential referred to in CP standards, where a depolarization of 30 mV from the open circuit potential is included. In the models, the open circuit potential used as boundary condition on the anodes is -1050 mV vs Ag/AgCl, which in reality is the closed circuit potential. For that reason, the anode potential during the simulations should be as close to -1050 mV vs Ag/AgCl as possible, since it is already assumed depolarized.

With a large anodic polarization slope, the change in anode potential is limited, since the anodes can deliver a large amount of current per volt change in potential. If the slope is small, the anodes will depolarize to a greater extent, which means that the driving voltage between the anode and the cathode will be lower, and hence, the anodes will be less effective, and a less

negative cathode potential is obtained, i.e. the cathode surface is less protected. In modelling, an anodic polarization slope of 100 $(A/m^2)/V$ is typically assumed based on modelling experience (*Table 5*). *Figure 12* shows a potential profile from Model 1, where 100 $(A/m^2)/V$ is used as slope in the anodic polarization curve, and as seen in the figure, the anode potentials does not deviate much from -1050 mV vs Ag/AgCl. The largest depolarization is present at Anode 1, with a value equal 6 mV. Hence, with a large anodic polarization slope as used in the models (100 $(A/m^2)/V$), closed circuit potential can be used as boundary condition for the anodes instead of the open circuit potential.

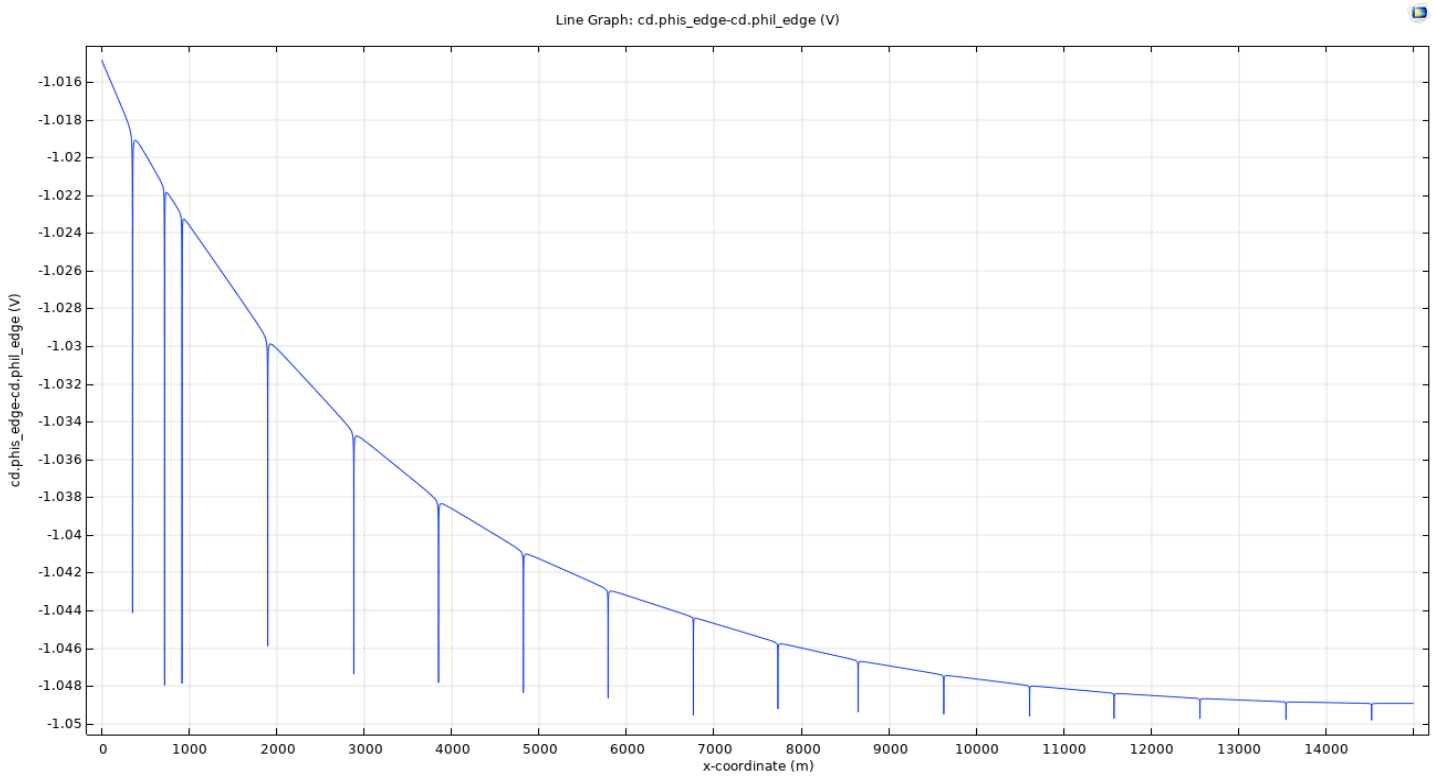

***Figure 12**, Drain profile of Model 1, where all the anodes have a potential equal to -1050 mV vs Ag/AgCl.*

5 Modelling Results

5.1 Sensitivity Study of the Well Geometry (Model 1)

The results from the sensitivity study of the geometrical parameters describing the drain point are represented as current drain profiles. Drain profiles showing absolute anode current output in addition to normalized curves are shown in *Figure 13* through *Figure 16*. The normalized current drain profiles show the percentage amount of current each anode deliver, which means that each anode current output is divided by the total amount of current drained by the well surface. The parameters investigated are the well depth, number of wells in the drain point and outer radius of the well casing. In addition, different slopes of the cathodic polarization curve have been investigated.

In *Figure 13a* through *Figure 15a*, it can be seen that when the geometrical parameters increase in value, i.e. the total surface area of the drain point increases, the amount of current drained increases. The current drained from the anodes closest to the drain point increases more than anodes further away from the drain point as the surface area of the drain point increases. All the geometrical parameters show the same effect on the drain profile as they are changed. As sees in *Figure 13b* through *Figure 15b*, where the percentage amount of current drained from the anodes is illustrated, it can be seen that the change in the drain profile as the geometrical parameters increases, is not present compared to *Figure 13a* through *Figure 15a*. As the total surface area of the drain point increases, and the total current drained increases, the percentage amount of current drained from each anode is constant. In *Figure 14b* and *Figure 15b*, only one curve can be seen, even though all the curves are plotted. The curves are identical as the parameters are changed.

The same effect can be seen in *Figure 16a* and *Figure 16b*, where the slope of the cathodic polarization curve is investigated. As the slope increases, the total amount of current drained increases, but the normalized curve shows that the percentage amount of current drained from each anode is constant and does not change as the cathodic polarization curve changes.

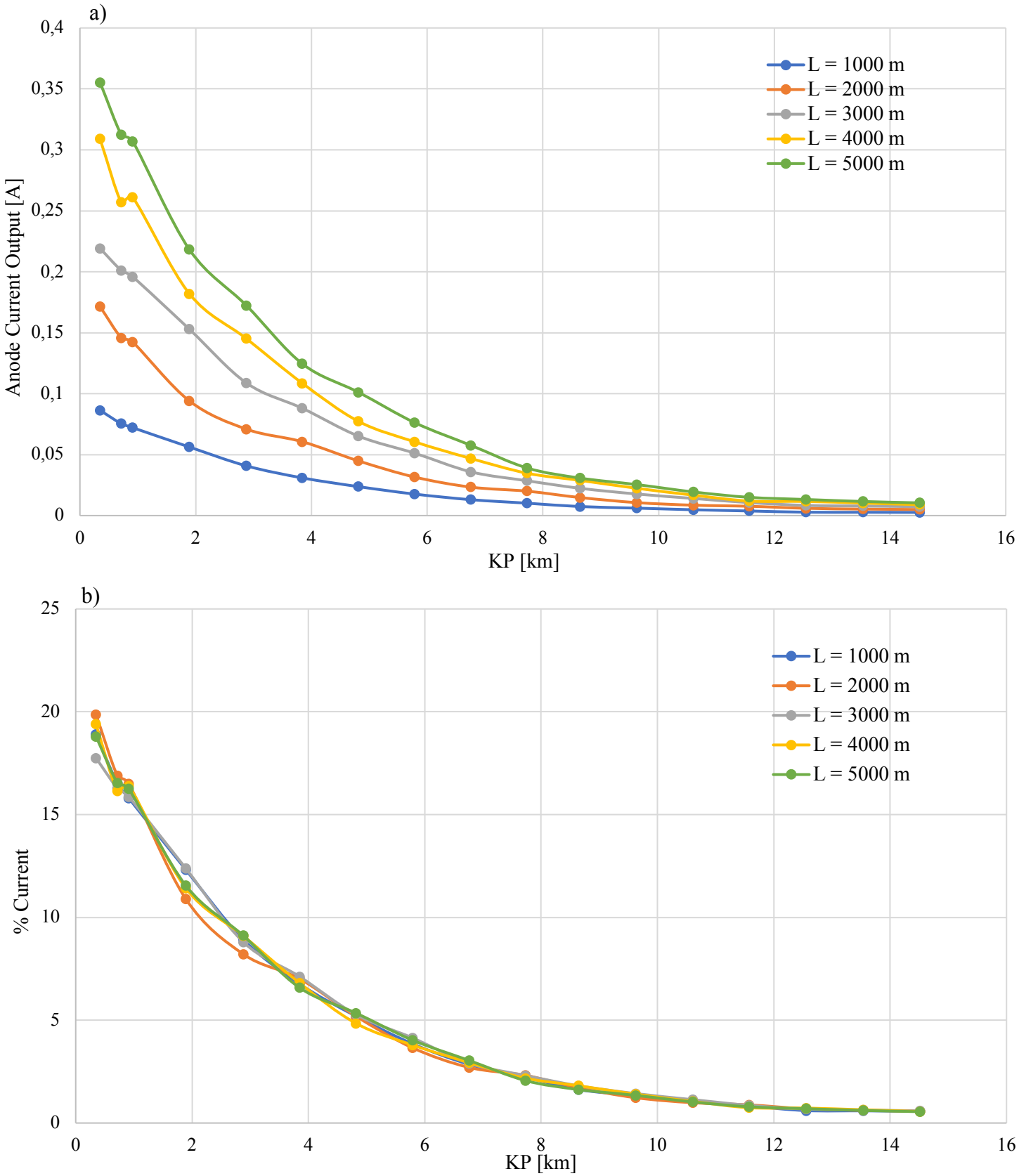

***Figure 13**, The effect of different well depths (L) on the drain profile. a) Drain profile showing the actual anode current output, b) normalized drain profile, showing % amount of current output of total current drained.*

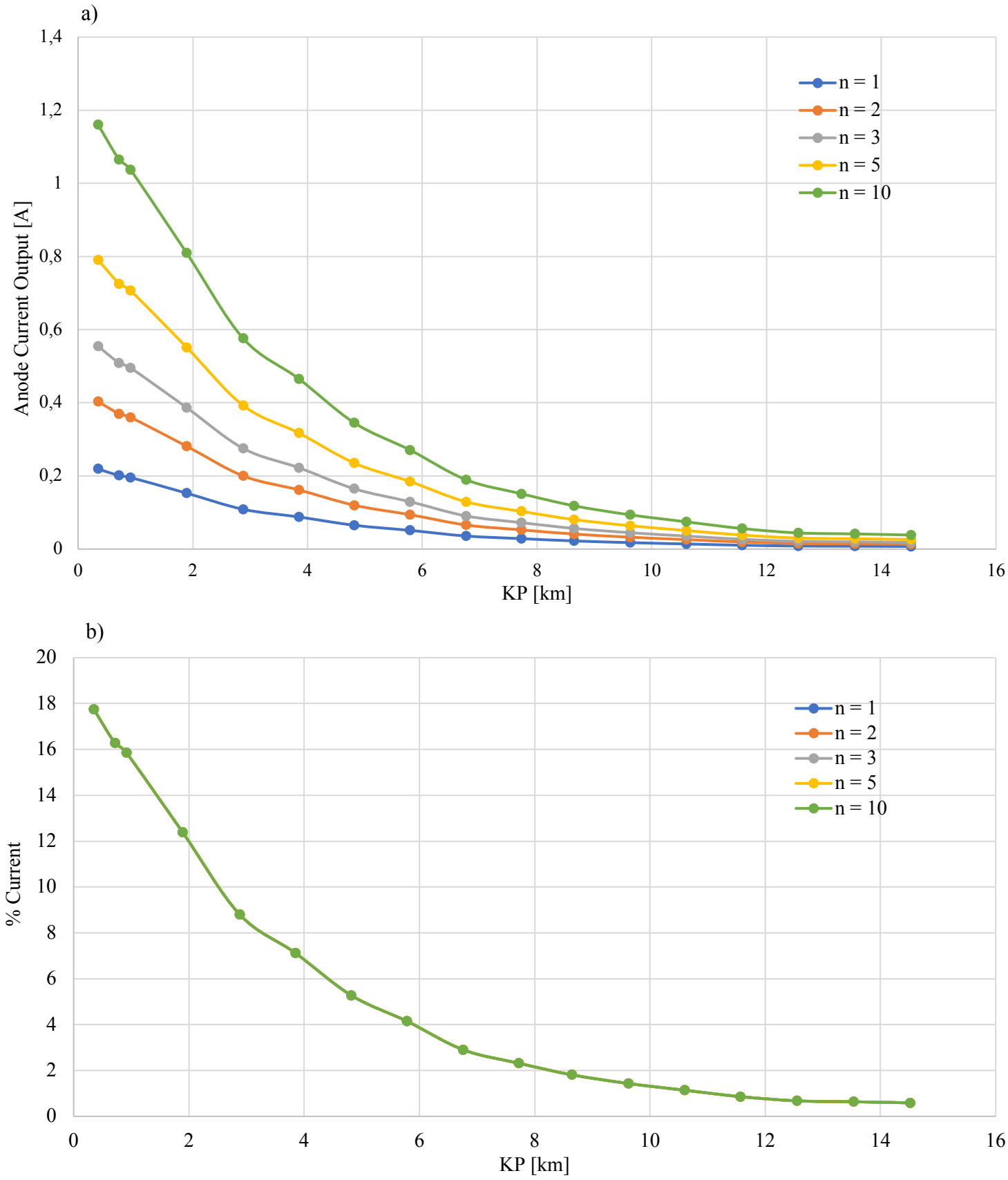

***Figure 14**, The effect of different number of wells (n) in the drain point on the drain profile. a) Drain profile showing the actual anode current output, b) normalized drain profile, showing % amount of current output of total current drained.*

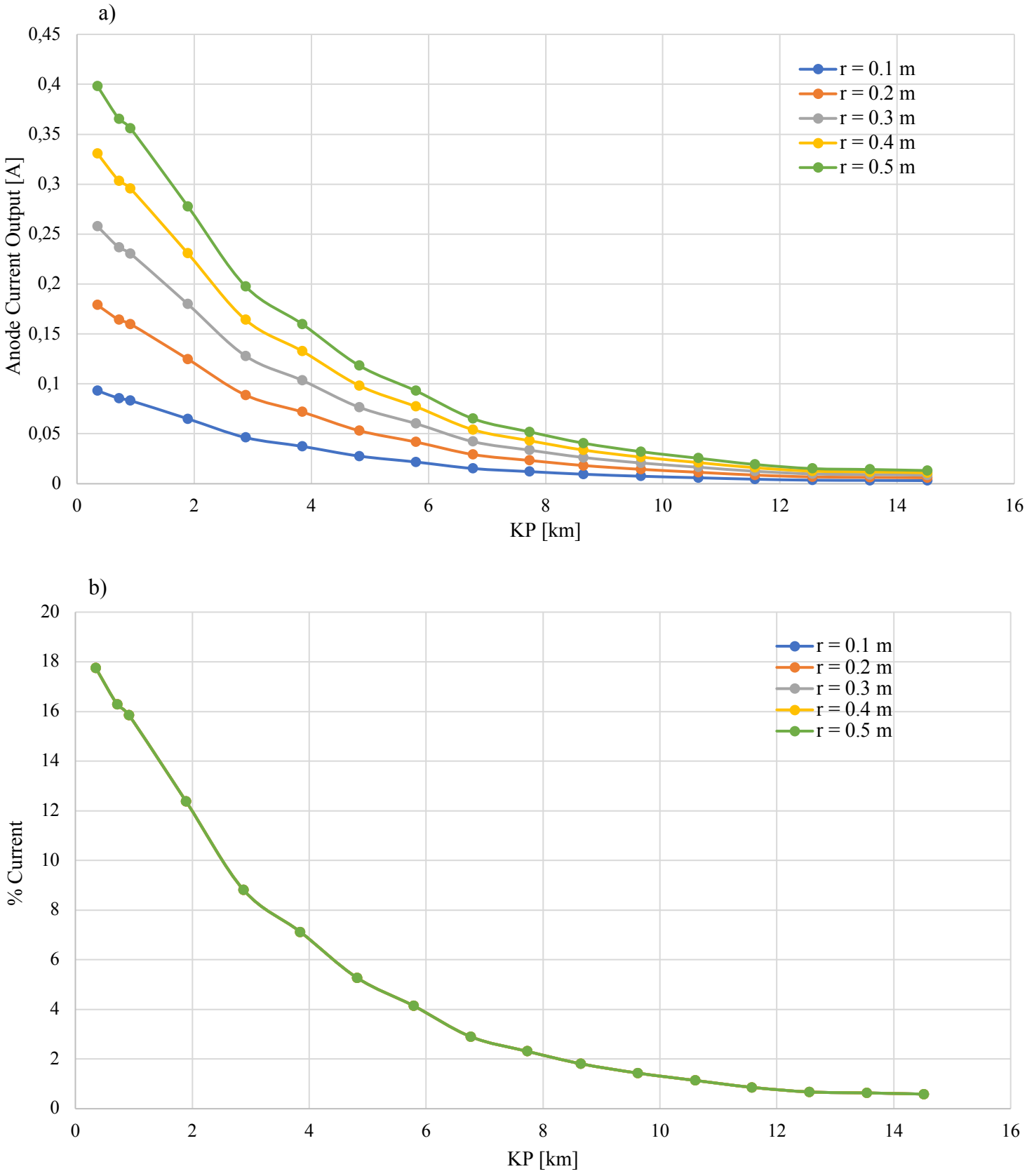

***Figure 15**, The effect of different well casing radius (r) on the drain profile. a) Drain profile showing the actual anode current output, b) normalized drain profile, showing % amount of current output of total current drained.*

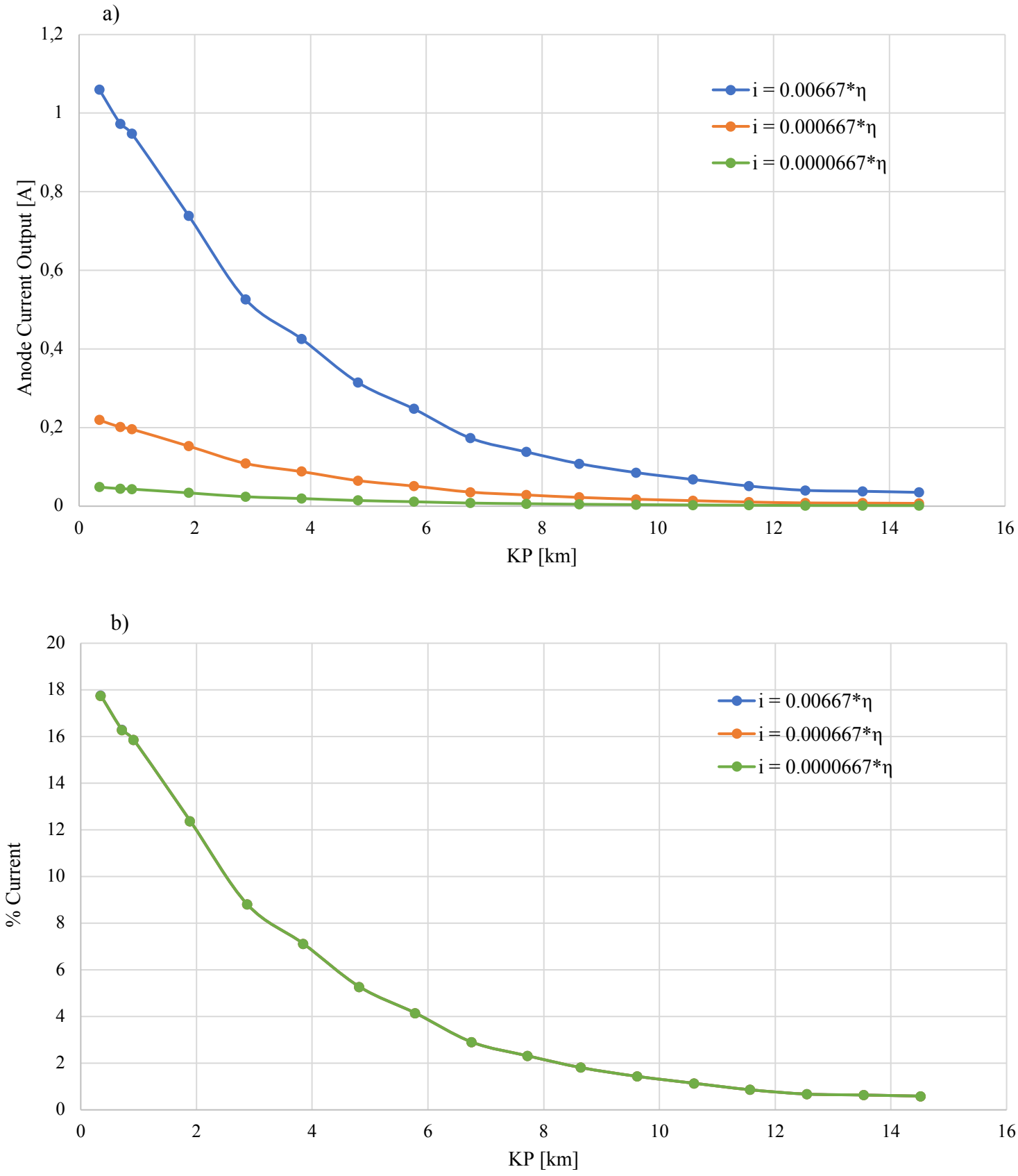

***Figure 16**, The effect of different polarization slopes on the well casing surface on the drain profile. a) Drain profile showing the actual anode current output, b) normalized drain profile, showing % amount of current output of total current drained.*

5.2 Rock dumped anodes vs. seawater exposed anodes (Model 1)

The results in *section 5.1*, all the anodes were seawater exposed since the well geometry was in focus. In reality, some of the anodes on pipe PP are rock dumped, more specific the anodes at KP 0.714 (Anode 2), KP 0.913 (Anode 3) and KP 6.760 (Anode 9). *Figure 17a* illustrates the drain profile when the anodes at KP 0.714, KP 0.913 and KP 6.760 are seawater exposed and rock dumped. *Figure 17b* shows the same result only normalized.

It can be seen in both *Figure 17a* and *Figure 17b* that when anodes are buried compared to seawater exposed, the drain profile changes significantly. The current output from the buried anode decreases, and the current output from the adjacent anodes increases. When only Anode 2 is buried, the effect of the adjacent anodes is not that significant, but when both Anode 2 and Anode 3 is buried, the current output of the first and the fourth anode increases to a great extent. The effect of Anode 9 when it is buried instead of seawater exposed, is limited to its own current output. Its current output is reduced as it is buried, but it does not affect the adjacent anodes significantly compared to the case when only Anode 2 and Anode 3 is buried.

As seen in *Figure 17b*, where the anode current outputs are normalized, buried anodes changes the percentage current output of the anodes, which is the opposite effect compared to the change in surface area of the drain point. The normalized curve in *Figure 17b* shows the same trend as the result in *Figure 17a,* which means that buried anodes affect the percentage amount of current the anodes supply to drain and is, hence, important to consider during modelling of CP systems.

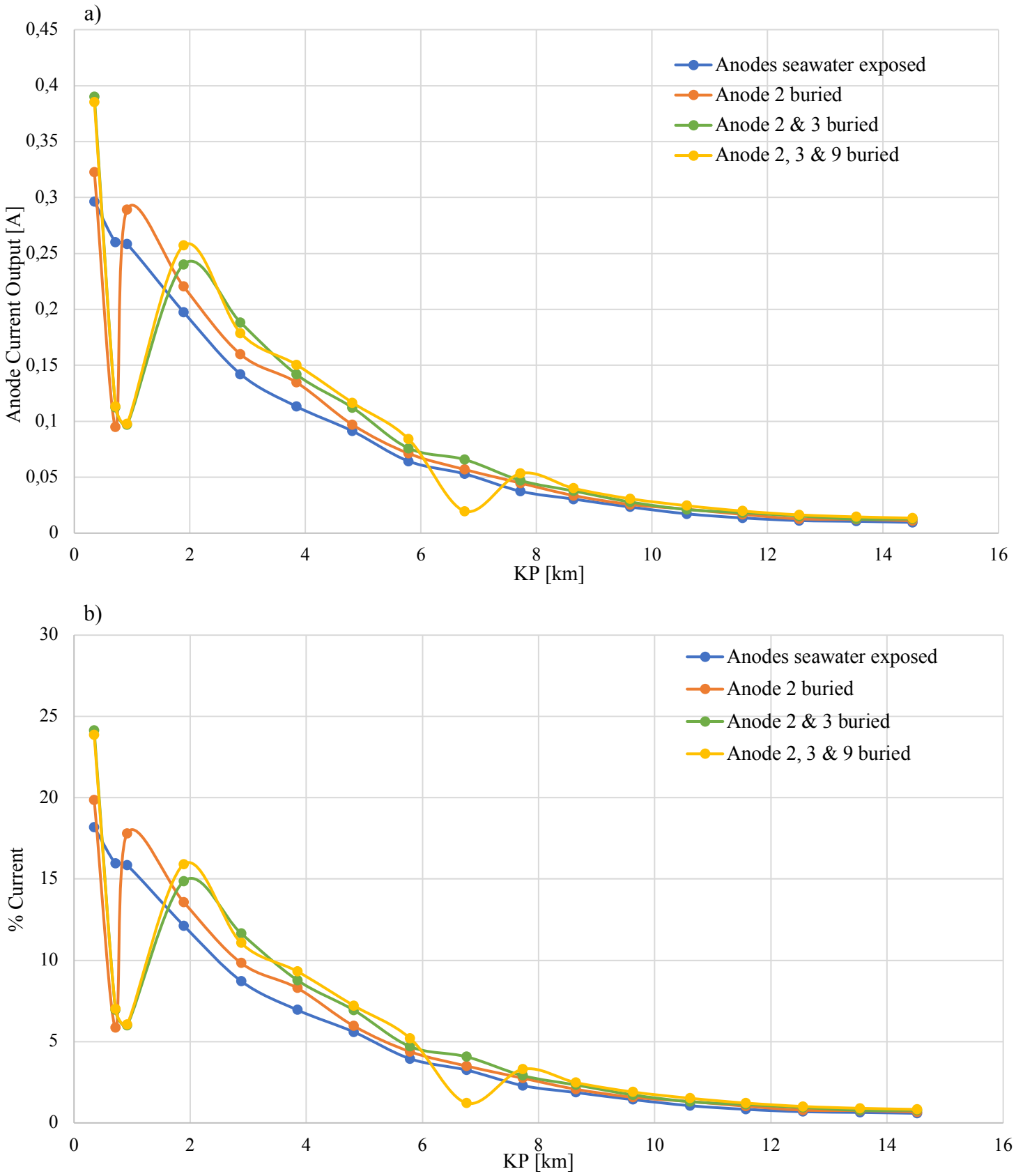

***Figure 17**, The effect of buried anodes on the drain profile. a) Drain profile showing the actual anode current output, b) normalized drain profile, showing % amount of current output of total current drained.*

5.3 Model Verification vs Survey Data (Model 3 and Model 4)

Since the effect of buried anodes showed a significant change in the percentage amount of anode current output supplied to drain, the anodes that are buried were included in Model 3 and Model 4. *Figure 18* compares the drain profile simulated in Model 1, Model 2 and Model 3 in addition to the measured drain profile, based on survey data, to Drain Point 1. It can be seen that the simulated drain profile from Model 3 is in good agreement with the drain profile simulated from Model 1 and Model 2. All the simulated drain profiles also match the shape of reference profile well, but the simulated anode current outputs are consistently lower compared to the anode current outputs from the survey data.

Figure 19 shows the result from Model 4 compared to the reference drain profile to Drain Point 2. It can be seen that the simulated drain profile matches the measured one very good, and the shape is almost identical with only a few deviations. Compared to Model 3, the drain profile from Model 4 is also consistently lower that the reference profile.

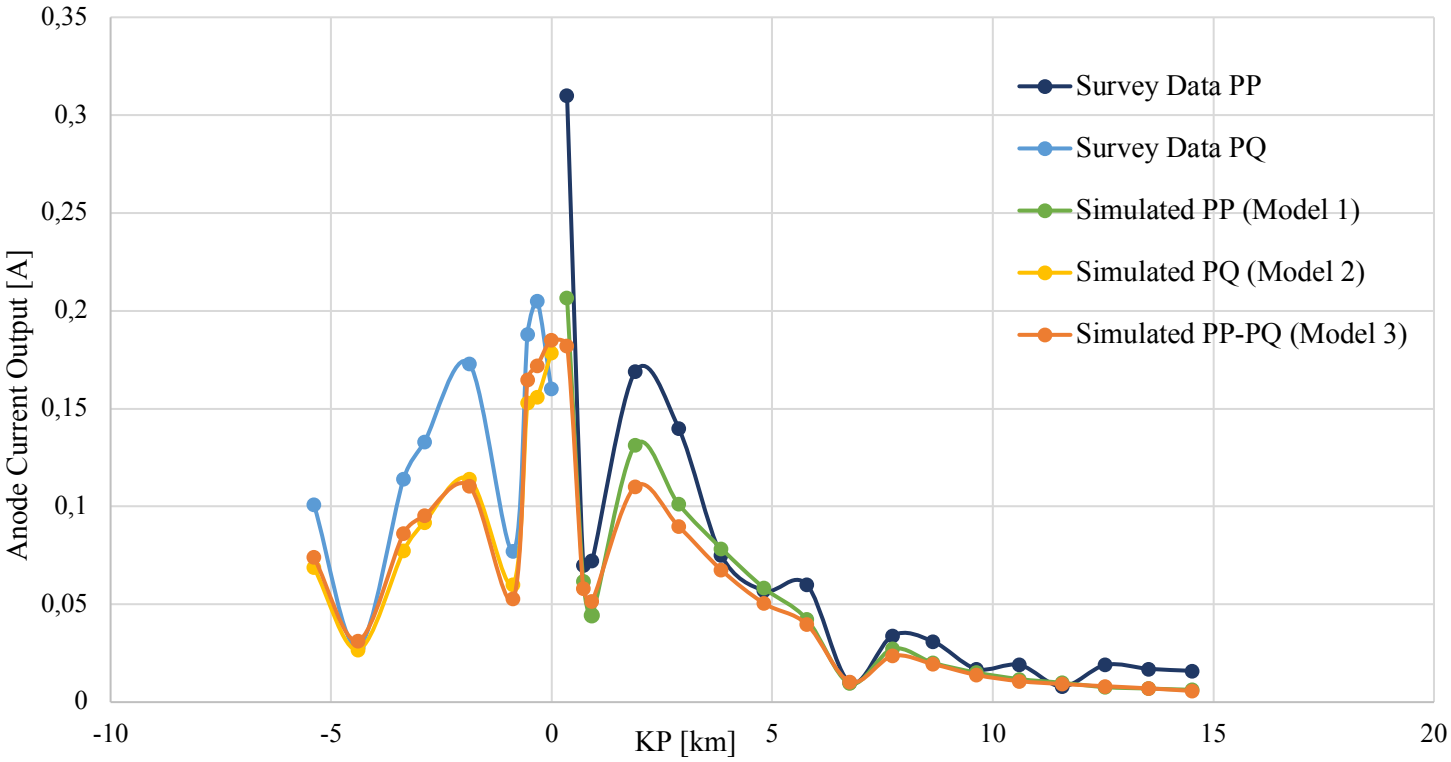

***Figure 18**, Simulated vs measured (survey data) current drain profiles from pipeline PP and PQ connected to Drain Point 1.*

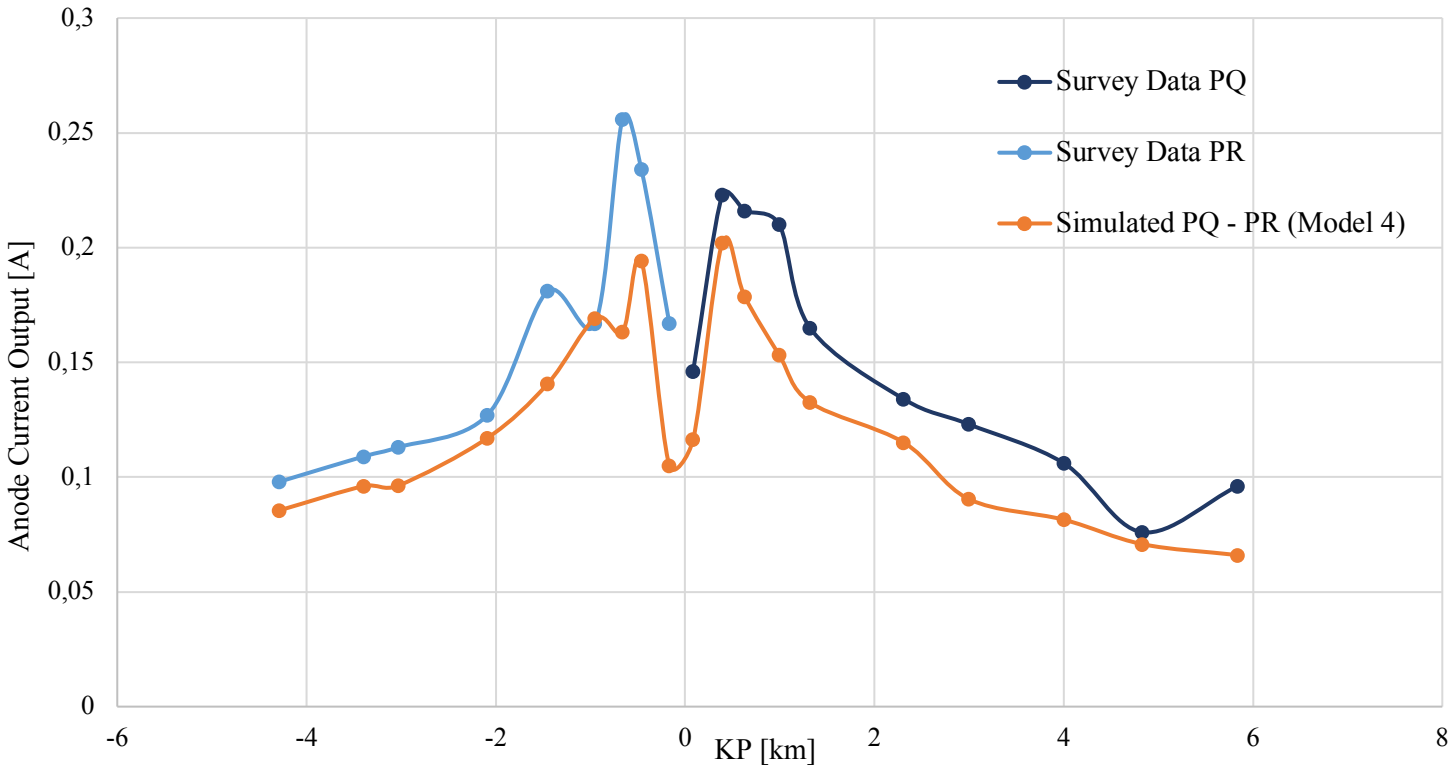

***Figure 19**, Simulated vs measured (survey data) current drain profiles from pipeline PQ and PR connected to Drain Point 2.*

5.4 Changes in Anode Distribution (Model 1)

Figure 20 shows how different anode configurations the first 1000 meters of the pipeline affect the drain profile. Model 1 is used with only seawater exposed anode. Simulations are performed with different combinations of anode distributions, where the second, the second and the third and all the first three anodes are removed. A simulation where the second and the third anode is removed, and the first anode is three times as large as the other anodes (Triple-Anode), is also performed.

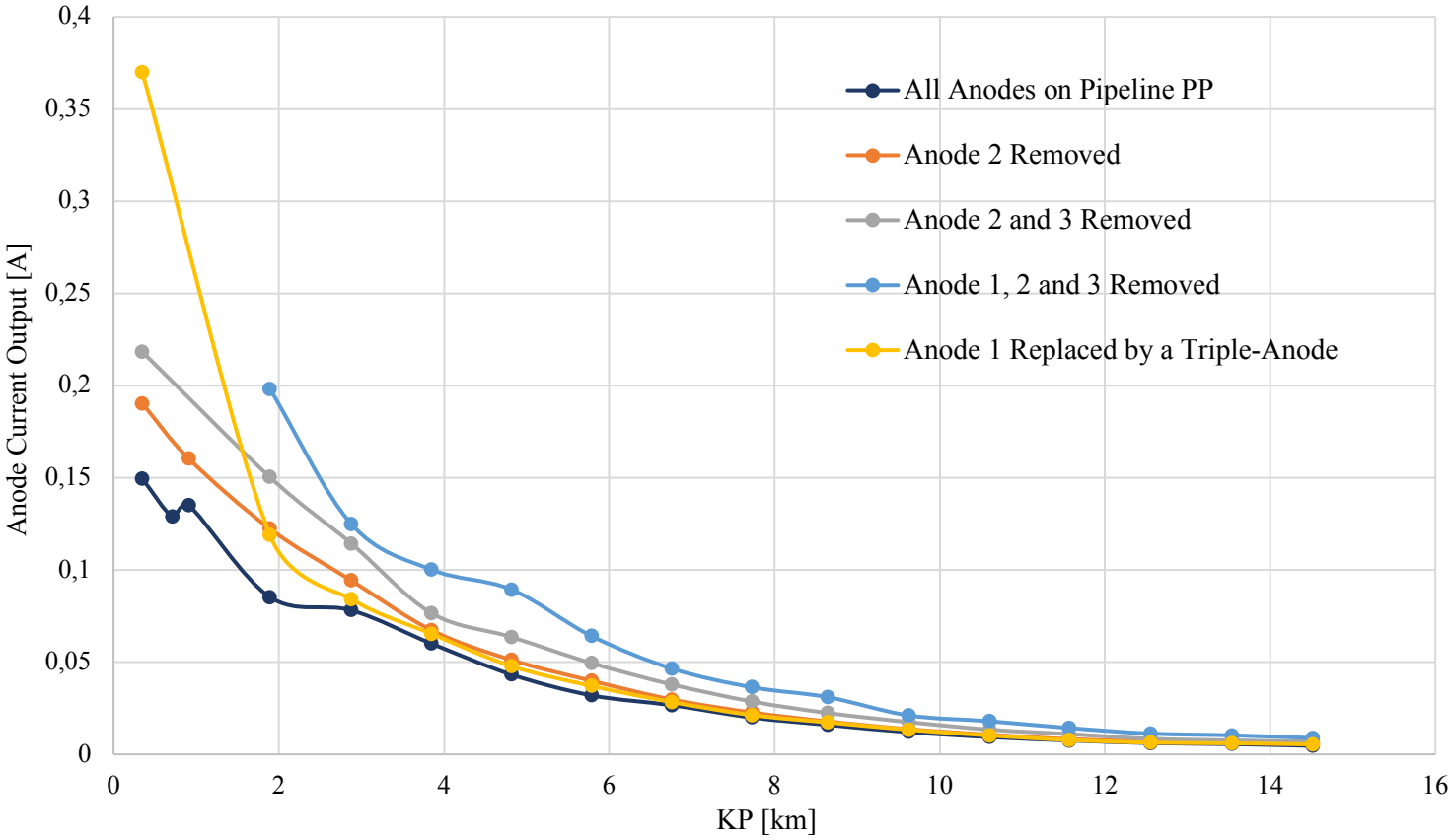

***Figure 20**, How different anode configurations in the first kilometer of the pipeline affect the drain profile. Model 1 is used with all the anodes seawater exposed.*

As seen in the *Figure 20*, all the different anode configurations change the potential profile. As anodes are removed, the current output of the anodes consequently increases. The most significant effect is when the three first anodes are replaced by the large triple-anode. The current output of that anode is much larger compared to the other anodes.

6 Discussion

In this chapter, the effect of the geometrical well parameters and buried anodes are discussed. The results are difficult to discuss against similar results, because similar publications are limited. In addition, some applications of the model developed are described to enlighten the opportunities and possibilities of the model developed.

6.1 The effect of geometrical parameters and Boundary Conditions

The geometrical parameters describing the wells, such as the depth, outer radius of the casing and number of wells in the drain point are important as they define the total surface area of the drain point that drains current. These parameters are not well known and may vary from casing to casing. For that reason, the importance of these parameters and how they affect the results, i.e. the drain profile from the simulations, are investigated.

The results of *Figure 13 through Figure 15* show that when the surface area of the well casing increases, either by increasing the depth (*Figure 13a*), the outer radius (*Figure 14a*) or the number of wells (*Figure 15a*), the current drain increases and hence the anode current output from the anodes in the drain zone. When these curves are normalized (*Figure 13b, Figure14b* and *Figure 15b*), the results show that the percentage amount of anode current delivered to the well surface does, however, not change with changing surface area, i.e. the distribution of anode current output along the pipeline (the drain profile) is not affected by the well geometry. The well can be modelled with a small radius or at large depth, but it will not affect the drain profile. As the number of wells in the drain point increases, the total surface area hence increases, and the anodes have to supply more current to the drain point. But as several wells are present, the cross-section area of the drain point also increases which allows more current to flow back. The well casing resistance will hence decrease, since more current can flow, and the current output from all the anodes will increase by the same factor. This is seen in the normalized curve (*Figure 14b*), where all the curves for the different number of wells in the drain point are identical. All the geometrical parameters change the resistance that all the anodes have in common, and not the resistance for individual anodes, and for that reason, the percentage amount of current supplied by the anodes cannot change as the geometry of the drain point changes. Since the surface area does not affect the drain profile, we cannot predict the total drain from the anodes installed on the pipeline, because the actual drain is dependent on the

real surface area of the drain point. However, these results show that it is possible to predict the distribution of anode current output along the drain profile (the pipeline).

Figure 16 shows how the polarization curve on the well surface changes the anode current output to drain and as seen in the normalized curve, the boundary condition does not change the percentage amount of current drained from the anodes either. The results are equal to the results regarding the geometrical parameters. This means that the slope of the cathodic polarization curve is dependent on the surface area of the well casings. In Model 2, 3 and 4, the well casing area is constant, and the same is the case for the slope of the cathodic polarization curve. If the surface area of the well casings was changed, the slope of the cathodic polarization curve would have been changed as well to correct for the change in cathodic surface area (well casings). Since the surface area of the drain point and its polarization curve does not change the anode's current distribution (%), the parameter of importance has to be the position of the anodes, which affect the resistance between the anode and the cathode.

When the well geometry and the boundary conditions on the well surface are of less importance regarding the drain profile, the parameter that affect the drain profile is the resistance between the anode and the cathode, and especially the metallic resistance in the pipeline. The total resistance between the anode and the cathode consists of several contributions: the resistance out of the anode (*equation 2.12*), the metallic resistance in the pipeline and the well casing (*equation 2.11*) and the electrolytic resistance. The resistance in the electrolyte and the well casing can be assumed equal for all the anodes, and the anode resistance is equal for anodes with the same depth of burial. In the models, the anodes are either half buried or completely buried (rock dumped anodes). The anode resistance for all seawater exposed anodes (half buried) will hence be equal, and the same for rock dumped anodes, which means that the metallic resistance in the pipeline is the only contribution to the total resistance that is different for the anodes. The metallic resistance is dependent on the position to the anode (the length away from the drain point), which is the parameter that is most important determining the percentage amount of anode current output. If the distance between the first and the second anode is increased, the resistance to the first anode is unchanged, but the resistance to the second anode increases as the pipe length between the anode and the drain point increases. According to Ohm's low (*equation 2.10*), when the resistance increases, the current output decreases. This

means that the anode position affects the amount of anode current output supplied to drain because it changes the relative resistance between the anodes.

In the study by Gartland and Bjørnaas [34], they studied, among other thing, the effect of well geometry on current drain to subsea wells, but they did not describe anything regarding results of the well geometry on drain to subsea wells in the report. Since the well geometry was a part of the study, but no results regarding the geometry was discussed, it may be because the results were insignificant and did not affect the current drained to the wells. If so, the results from Model 1 in *section 5.1* agrees with the results from Gartland's and Bjørnaas' study. However, it is difficult to compare the results from *section 5.1* to the study by Gartland and Bjørnaas, since none of their results regarding the well geometry are presented.

6.2 The effect of buried anodes on the drain profile

Figure 17a and *17b* show how the drain profile is affected by rock dumped anodes compared to when all anodes are seawater exposed. The percentage amount of current drained from the anode at KP 0.714 is reduced from approximately 16 % to 6 % when it is considered rock dumped instead of seawater exposed. The amount of current output from the adjacent anodes increases, but only with a few percent. When the anode at KP 0.913 is in addition considered rock dumped, the current output from the first anode increases from 20% to approximately 24%, and the other anodes further away from the well also get an increase in current output. When the anode at KP 6.76 is in addition to the two other rock dumped anodes considered rock dumped, there are only local changes to that specific anode that is significant, the other anodes are not affected that much. The reason may be because that anode has a low current output in the first place and is of less importance regarding drain to the well.

The reason anodes deliver less current when they are rock dumped compared to seawater exposed is due to the conductivity. Seawater has a conductivity of 3.33 S/m [7] while the conductivity of a rock dump is rather unknown, but it is for sure lower than seawater due to the conductivity of rocks and other sediments. When parts of the environment surrounding anodes changes, in this case the medium above the anode, the anode resistance also changes. The anode resistance is calculated by McCoy's equation (*equation 2.12*), where the environment resistivity is a parameter. For partly buried pipelines, the environment is heterogenous, consisting of two different mediums. The equivalent anode resistance can be calculated by the equivalent circuit

resistance of a parallel circuit where the resistance to seawater is one resistance and the resistance to sediment is the second resistance. When seawater is replaced by a rock dump, the resistance to the rock dump increases compared to seawater and hence the equivalent anode resistance. The total resistance from the anode to the cathode, as described in the previous section, is depending on the anode resistance, the resistance in the electrolyte and the metallic resistance in the well casing and the pipeline. When one of these individual resistances increases due to a decrease in conductivity, the total resistance increases and hence the current output from an anode decreases. This explains why rock dumped anodes deliver less current than seawater exposed anodes, and why it is important to consider them rock dumped instead of just buried in sediment, since the difference in conductivity of rocks and sediment is significant.

As seen in the results (*Figure 12*), the effect of rock dumped anodes plays a significant role in the drain profile, which means that rock dumped anodes have to be included in a realistic model. If they are only considered seawater exposed or buried in sediments as all other anodes to simplify the model, the slope of the drain curve is lower and the current output from the anodes adjacent to the rock dumped ones is several percentages lower compared to the result when all the three anodes are rock dumped.

6.3 Model Verification

The drain profiles for pipe PP and PQ (Model 1, 2 and 3) are shown in *Figure 18*. The measured data includes the anode current output to both drain and the current supplied to the pipeline surface. The simulated curves only consider drain to the well casing surface and is the reason why it is a difference between the simulated and the measured curves. Despite the difference between the measured and simulated curve, the overall shape of the curves match, but there are some exceptions of individual anodes where the deviation is larger compared to other anodes. The reason for the large deviation for some anodes may be because the model handles all the anodes with equal depth of burial. This is not a realistic case and some anodes may have smaller or larger burial depth which will cause large deviations between the simulated and measured data. An extremely detailed model with respect to burial of all the anodes would have been necessary if the curves should have matched perfectly, but despite the individual deviations, the shape of the curves match good.

Another reason for large, individual deviation, in addition to different burial depths, is that the consumption of anodes may play an important role. Some anodes may be more consumed than others during the survey of the pipeline and hence, the measured result will give a low current output. In the model, all anodes are considered new and equal in size, which means that they will deviate more from anodes that are largely consumed than anodes that are not.

Since the simulated drain profile in Model 3 matches good with the measured data, the model is verified by simulating the drain profile from Model 4. The values of the parameters are equal, the only thing that is different is the anode position and the length of the pipelines. *Figure 19* shows the result from Model 4, and the drain profile matches the measured one good. There are less large, individual deviations and the shape is almost identical. The difference between the curves is in this case as well due to that the simulated drain profile only considers drain to the well and not the current delivered to the pipeline surface.

If the pipeline was included in the models, the anode current output would have been supplied to both the well casings and the pipeline surface. It then would have been necessary to estimate the current supplied to only the well casings. A necessary assumption would have been that all anodes supply an equal amount of current to the pipeline surface based on the current density on the surface of the pipeline, and hence the anode current supplied to the well casings could have been estimated by subtracting the current supplied to the pipeline from the total anode current output for each anode. The results when drain to the pipeline is included would have been less accurate since an assumption would have been made to obtain the drain profile along the pipeline from drain to only the well casings. The most realistic results are hence obtained by neglecting the current supplied to the pipeline and only considering the current drained by the well casings.

6.4 Applications of the Model

Since the results in *Figure 18* and *Figure 19* were positive, the model can be used as a tool to simulate current drain to subsea wells. A model like this one can have several applications that provide useful information regarding drain to subsea well and about the CP system the well drains current from.

6.4.1 Anode Distribution

Anode distributions are designed according to CP design standards, as DNV-RP-F103 ISO 15589-2 [5,7]. According to both these standards, an anode distance of 300 m is recommended. This distance will ensure sufficient anode current output in the event of an adjacent anode being lost such that the actual distance becomes 600 m.

The CP design on the pipelines investigated appear to agree with ISO 15589-2:2004. The latest revision of ISO 15589-2 is from 2012, but no changes regarding anode spacing was made compared to the 2004 revision. The general anode distance is approximately 1000 m, with some safety factor on the anode spacing the first and final 1000 m of the pipelines. The anode spacing is larger that 300 m, but if calculations have been made that justifies the anode distribution, 300 m can be exceeded. The safety factor is confirmed in the standard and is justified by the possibility of increased coating damage close to the ends of the pipeline, increased current drain and because the pipeline anodes adjacent to the structure may also provide current to the structure.

Different anode distribution the first 1000 m of pipe PP (Model 1) is shown in *Figure 20*. Simulations where the second, the second and the third, and all the three first anodes are removed are performed to see how the lack of safety anodes affect the drain profile. As seen in *Figure 20*, as the second and the third anode are removed, the current output from the adjacent anodes increases, but the length of the drain zone in not affected significantly. The anode that is affected the most by the removal of anodes on the first 1000 m, is the first anodes. Compared to when all anodes are present, when both the second and third anode are removed, the anode current output from the first anode increases by approximately 8%. If this result is compared to the result when all the three first anodes are removed, we see that the fourth anode, which then becomes the first anode on the pipeline, has a lower current output than the first anode when only the second and third anode is removed. This means that if the safety anodes are not included in the CP design, hence the second and the third anode in this case, the loss of the first anode by damage or that it is fully consumed, will not be critical for the CP system and the other anodes, because the amount of current drained from these anodes will not increase significantly when the first anode is lost.

Another possible case regarding the anode distribution, is that the safety anodes in the first 1000 m can be replaced by one large triple anode close to the structure. This large anode will be able to provide a large amount of current to drain, which is shown in *Figure 20*. The triple anode supplies 44% of the total current drained to the well surface. Since it is larger than the other anodes and it is the anode located closest to the well, it will partly shield the other anodes, which will have a much lower anode current output compared to the triple anode. When this anode is consumed, the case will be equal to when all the anodes in the first 1000 m are removed, which is also shown in *Figure 20* and discussed in the section above. It will not be critical for the other anodes, because after the increase in current output, the current output is less compared to the case when the second and third anode is removed. In addition, they have been less consumed due to the low current output with the triple anode present and hence the lifetime of the remaining anodes could be increased when a large triple anode is used that can be consumed.

If that result in combination with the result when the three first anodes where removed, CP design could be reconsidered in light of the safety factor for anode distribution. The extra anodes installed can be replaced by a triple anode that will dominate the current output to drain. Due to the large anode current output, this anode will be consumed first, and when it does, the current output from the remaining anodes will increase, but it will be lower compared to the case when the first anode is equal in size to the other anodes and the second and third anode in removed. As a result, the loss of the first anode will not be critical for the other anodes and the need of safety anodes in the first 1000 m of the pipe is probably not as necessary as thought.

6.4.2 Anode Monitoring

To be able to calculate and predict drain to subsea wells from the CP system of pipelines, a survey has to be performed where the anode current output is a result. From these results, a drain profile can be estimated to see how much current the anodes deliver to drain and how long the drain zone is. An alternative to this method is the use of anode monitoring, as described in *section 2.2.3*, of one anode only, in combination with the use of modelling. An instrument box can be connected to one anode in the drain zone, as the third anode for example. It may not be desirable to connect the monitoring box to the first anode, because it is often very close to the template structure, which is often rock dumped or interference to the template anodes could affect the anode output of the first anode. A seawater exposed anode further away can instead

be used as monitoring anode. The instrument box can be designed to provide anode current output data that do not require survey equipment or the use of personnel. By knowing the number of anodes and their position along the pipeline, the drain profile can be modelled, and hence information regarding the current output from all the anodes can be obtained.

From the previous results, the well geometry is of less importance when it comes to how the drain profile is. With lack of information regarding the well geometry, these parameters can just be assumed. The polarization curve can be decided by a simple iteration process, since when the well geometry is assumed, it is the only unknown parameter left. This way, the model developed in this project can easily be used determining the drain profile by matching the current output by the simulated anode with the monitored anode.

When using the model developed without knowledge of the current output for all the anodes and hence the amount of current drain, the symmetry factor for the polarization curve has to be assumed since there are no survey data available to calculate it from. If the well contains two incoming pipelines, the symmetry factor can be assumed to be two, which means that the well drains an equal amount of current from each pipeline. If only one incoming pipeline is present, the symmetry factor can be set to one. The assumptions regarding the symmetry factor is fair and can be approved by the values calculated for Model 3 and Model 4 in *Table 5*, where in both cases there are two incoming pipelines present and the symmetry factor is close to two.

By simulating the drain profile on the basis of only one known anode current output, the need of pipe surveys where all the anode current outputs are measured becomes less important, which can be very helpful in an industry where cost savings is a major driving force.

6.4.3 Summary of the model's possibilities

Both the applications of the model described can contribute to cost savings in an industry where cost is a major driving force. If this model, with some further development, can contribute to change the requirements in CP design for anode distributions on pipelines, it would contribute to save costs due to reduced number of anodes needed to be installed.

It will also save costs when it comes to the use of monitoring only one anode and use the model for determining the drain profile of the other anodes, since the need for anode measurements is reduced which reduced the time needed for a pipeline survey. If a pipeline is well coated and it is known that the coating doesn't have any significant damages, the need for a pipeline survey may not be necessary at all to be able to determine the current drain from the pipeline to the adjacent well, and that can save the industry for a lot of expenditures.

7 Conclusion

- The parameters defining the well geometry, as well depth, outer radius and number of wells, which all affect the surface area of the well structure, does not change the percentage amount of current drained from the connected pipeline's anodes.

- The boundary conditions on the well casing surface, as the polarization curve does not affect the percentage amount of current drained from the connected pipeline's anodes. Thus, a general cathodic polarization curve used for the well casing surface does not exist, since the slope of the polarization curve has the same effect on the current distribution (%) from the anodes as the geometry of the well casing. The slope is dependent on the surface area, and as the surface area of the well casings changes, the anodic polarization slope also has to be changed.

- The anode current output to drain is dependent on the location of the anodes on the pipeline, due to changes in the resistance between the anodes and the cathode (well casing surface). Thus, the location of the anodes is the most important parameter affecting the current distribution (%) from the pipeline's anodes.

- By building a realistic model with respect to the position of the anodes and considering rock dumped anodes rock dumped instead of buried in sediment, the simulated current drain profile matches a measured drain profile from a pipeline survey relatively good.

- The total amount of current drained from the anodes installed on the pipelines cannot be predicted without exact information of the drain point geometry. However, the current distribution (%) from the anodes can be predicted without knowing the exact geometry of the drain point.

8 Suggestions for Further Work

According to the literature, the effect of different soil layers can affect the potential profile along a subsea well and hence the current it drains. Mapping the type of sediments with depth at Field A will give more information regarding the conductivity of the electrolyte and hence a more accurate model can be built. Mapping at this scale will require a lot of resources, but a better understanding of the drain to subsea wells could be obtained, which can be valuable for improving the knowledge and for other CP simulations regarding drain.

The simulations performed in this master's thesis is stationary with respect to time, i.e. the time is stagnant at year zero. A time simulation from year zero to the end of the design lifetime can give information on how the current drain changes with time. This can provide information on how the polarization of the well surface evolves from one time to another. If the current drain is reduced so much with time that it can be neglected as the time approached the end of the design life of the pipelines CP system, it can affect the need of CP retrofit to a great extent. But if the drain is almost as high at year 20 as it is at year 1, the need of CP retrofit is more important. Such knowledge of the evolution of the drain with time is valuable when it comes to CP design and CP retrofit.

9 References

[1] L.J. Alveberg, E.V. Melberg, (2013). Facts 2013: The Norwegian Petroleum Sector. *ISSN, pp.20*.

[2] P. Marcassoli, A. Bonetti, L. Lazzari, M. Ormellese, (2014). Modeling of Potential Distribution of Subsea Pipeline under Cathodic Protection by Finite Element Method. *Materials and Corrosion 2015, 66, No. 7*.

[3] J. Britton, (1999). The Role of Cathodic Protection in Offshore Pipeline Integrity. *Deepwater Corrosion Service.*

[4] DNV-RP-B401, (2017). Cathodic Protection Design. *Det Norske Veritas*.

[5] DNV-RP-F103, (2010). Cathodic Protection of Submarine Pipelines by Galvanic Anodes. *Det Norske Veritas*.

[6] NORSOK M-503, (1994). Common Requirements Cathodic Protection.

[7] ISO 15589-2, (2012). Petroleum, Petrochemical and Natural Gas Industries – Cathodic Protection of Pipeline Transportation Systems – Part 2: Offshore Pipelines. *International Organization of Standardization*.

[8] W.H. Hartt, D. Lysogorski, H. Qian, K. Bethune, P. Pierson, (2001). Retrofit cathodic Protection of marine pipelines associated with petroleum production. *Center of Marine Materials – Florida Atlantic University.*

[9] D. Lysogorski, (2001). Cathodic Protection Modelling of Marine Pipelines. *Thesis – Florida Atlantic University.*

[10] R.A. Adey, (2006). Modelling of Cathodic Protection Systems. 12th edition. *WIT Press*

[11] S. Elbeik, A.C.C. Tseung, A.L. Mackay, (2003). The Formation of Calcareous Deposits During the Corrosion of Mild Steel in Seawater. *Chemical Energy Research Center – The City University, London.*

[12] Y. Yang, J.D. Scantlebury, E.V. Koroleva, (2015). A Study of Calcareous Deposits on Cathodically Protected Mild Steel in Artificial Seawater. *School of Materials, the University of Manchester.*

[13] S. Røstbø, (2016). Cathodic Protection of Steel-Aluminum Galvanic Couples for a New Generation Lightweight Subsea Structures. *Master Thesis – NTNU.*

[14] F. Varela, M. YJ. Tan, M. Forsyth, (2016). An Overview of Finite Element Models Used for CP Applications. *Institute of Frontier Materials, School of Engineering, Deakin University, Australia.*

[15] T. Okstad, Ø. Rannestad, R. Johnsen, K. Nisancioglu, (2007). Significance of Hydrogen Evolution During Cathodic Protection. *NACE International.*

[16] United States Naval Academy, (1996). Cathodic Protection Design.

[17] G.H. Backhouse, (1981). Recent Advances in Cathodic Protection Surveys of Subsea Pipelines. *Society of Petroleum Engineers*.

[18] ISIS. Guidelines for Subsea Pipeline Cathodic Protection Survey, accessed 25 November 2018, < http://www.ises.tech/wp-content/uploads/2013/06/Guidelines-for-Subsea-Pipeline-Cathodic-Protection-Survey.pdf >

[19] V. Chaker, J.D. Palmer, (1989). Effects of Soil Characteristics on Corrosion. *ASTM.*

[20] G.Ø. Lauvstad, M. Bjørnstad, H. Osvoll, (2017). Impact of rock dump on CP design for offshore structures and pipelines. *Force Technology*.

[21] J.P. La Fontaine, T.G. Cowin, J.O. Ennis, (2000). Cathodic Protection Monitoring of Subsea Pipelines in the Arctic Ocean. *Deepwater Corrosion Service.*

[22] R. Montoya, O. Rendòn, J. Genesca, (2005). Mathematical Simulation of a Cathodic Protection System by Finite Element Method. *Materials and Corrosion, 56, No. 6.*

[23] B. Nistad, (2016). The Boundary Element Method Simplifies Corrosion Simulation. *Comsol blog.*

[24] C. Andrade, C. Alonso, M. Acha, M. Castellote, (1996). Experimental Comparison Between Chloride Diffusion and Migration Tests in Steady-State Condition. *NACE International.*

[25] P. Miltiadou, L.C. Wrobel, (2002). A BEM-based Genetic Algorithm for Identification of Polarization Curves in Cathodic Protection Systems. *Department of Mechanical Engineering, Brunel University, Uxbridge.*

[26] R. Adams, (2013). Calculus 2, 8th edition. *Pearson, pp.921-924.*

[27] J.F. Yan, S.N.R. Pakalapati, T.V. Nguyen, R.E. White, R.B. Griffin, (1992). Mathematical Modelling of Cathodic Protection Using the Boundary Element Method with a Nonlinear Polarization Curve. *The Electrochemical Society*.

[28] R.A. Addey, C.A. Brebbia, S.M. Niku, (1990). Application of Boundary Elements in Corrosion Engineering. *Topics in Boundary Element Research, vol. 7, pp.38-41.*

[29] C.H. Lim, (2014). Butler-Volmer equation. *Lecture notes.*

[30] J. Zhang, Y. Du, M. Lu, (2012). Numerical Modeling of Cathodic Protection Applied to Deep Well Casings. *Institute of Advanced Materials and Technology, University of Science and Technology Beijing.*

[31] C. Li, M. Du, J. Sun, Y. Li, F. Liu, (2013). Finite Element Modeling for Cathodic Protection of Pipelines Under Simulating Thermocline Environment in Deep Water Using a Dynamic Boundary Condition. *Journal of The Electrochemical Society.*

[32] D. Min, W. Huanhuan, H. Shouzhi, G. Rongjie, Y. Dan, (2018). Finite Element Modeling of Cathodic Protection of Well-Casing Through Seawater, Sea Mud and Rock. *NACE International.*

[33] S.M. Wigen, H. Osvoll, M. Gouriou, (2013). CP of Offshore Jacket by Remote Anode Sleds and Discussion About Current Drain to Buried Structures. *NACE International.*

[34] P.O. Gartland, F. Bjørnaas, (1998). Computer Modeling Studies of Current Drain to subsea Wells in the North Sea. *NACE International*.

[35] Norsk Petroleum, (2019), accessed 28 April 2019, < https://www.norskpetroleum.no/fakta/felt/ >

[36] Cescor. Inspection and Survey, accessed 22 November 2018, < http://www.cescor.it/en/what-we-do/cathodic-protection-inspection.html >

[37] L. Taraldsen, (2014). Denne sensoren kan "se" ørsmå rørskader på 3000 meters dyp. *TU.no*

[38] < https://www.comsol.com >

[39] NACE SP0176, (2007). Corrosion Control of Submerged Areas of Permanently Installed Steel Offshore Structures Associated with Petroleum Production. *NACE International.*

[40] B. Bazzoni, M.C. Briglia, (2006). Cathodic Protection of Well Casings in the Attahaddy Gas Field. *NACE International.*

[41] Deepwater Corrosion Service Inc, (2019), accessed 23 May 2019, < https://stoprust.com/products-and-services/bracelet-anodes/

Appendix A: Calculation of current supplied to drain in *Table 1*

The total amount of anode current output of the different pipe sections (PP_1, PQ_1, PQ_2 and PR_2) is the sum of each anode output. The surface area of the different pipe sections is according to the parameters in *Table 2*.

***Table A1**, Surface area of the pipe sections.*

Pipe section	Surface area [m^2]
PP_1	18849.6
PQ_1	6911.5
PQ_2	7791.1
PR_2	5654.9

With a constant current density on the surface of the pipelines, the current supplied to the pipelines is calculated by multiplying the current density on the pipelines by the surface area (*equation 2.7*). The amount of current from each pipe section supplied to the well casings is hence calculated by subtracting the current supplied to the pipelines from the total amount of anode current output.

***Table A2**, Total anode current output, current supplied to the pipeline surface and current supplied to the well casings (drain).*

Pipe section	Total Current Output	Current to Pipeline	Current to Drain
PP_1	1.124 A	0.377 A	**0.747 A**
PQ_1	1.179 A	0.138 A	**1.041 A**
PQ_2	1.495 A	0.156 A	**1.339 A**
PR_2	1.452 A	0.113 A	**1.339 A**

The column to the right in *Table A2* is the current supplied to drain from each pip section and is the values listed in *Table 1*.

Appendix B: Derivation of *equation 2.4* from Laplace equation [28]

Laplace equation represents the flow of current in a uniform, isotropic medium, i.e. the electrolyte.

$$\kappa \nabla^2 E = 0 \tag{B.1}$$

$$I_{x_i} = \frac{1}{\kappa}\frac{\partial E}{\partial x_i} \tag{B.2}$$

The boundary conditions over Γ is described as A.3 where $\bar{E}$ and $\bar{I}$ are known and Γ_1 and Γ_2 are parts of the complete boundary Γ.

$$E = \bar{E} \quad on\ \Gamma_1$$
$$I = \bar{I} \quad on\ \Gamma_2 \tag{B.3}$$

A.1 can be solved numerically from the weighted residual statement, where E^* is the weighted function and I^* as described in equation A.5.

$$\int_\Omega \nabla^2 E(x) E^*(y,x)\, d\Omega(x) = \int_{\Gamma_2} [I(x) - \bar{I}(x)] E^*(y,x) d\Gamma(x) - \int_{\Gamma_1} [E(x) - \bar{E}(x)] I^*(y,x) d\Gamma(x) \tag{B.4}$$

$$I^* = \frac{\partial E^*(y,x)}{\partial n(x)} \tag{B.5}$$

A.4 can be integrated by part with respect to x_i

$$-\int_\Omega \frac{\partial E(x)}{\partial x_i}\frac{\partial E^*(y,x)}{\partial x_i} d\Omega(x) = -\int_{\Gamma_1} I(x) E^*(y,x) d\Gamma(x) - \int_{\Gamma_2} \bar{I}(x) E^*(y,x) d\Gamma(x) - \int_{\Gamma_1} [E(x) - \bar{E}(x)] I^*(y,x) d\Gamma(x) \tag{B.6}$$

Integrating by part again gives the general equation A.8

$$\int_\Omega \nabla^2 E^*(y,x) E(x)\, d\Omega(x) = -\int_{\Gamma_1} I(x) E^*(y,x) d\Gamma(x) - \int_{\Gamma_2} \bar{I}(x) E^*(y,x) d\Gamma(x) + \int_{\Gamma_2} E(x) I^*(y,x) d\Gamma(x) + \int_{\Gamma_1} \bar{E}(x) I^*(y,x) d\Gamma(x) \tag{B.7}$$

$$\int_\Omega \nabla^2 E^*(y,x) E(x)\, d\Omega(x) = -\int_\Gamma I(x) E^*(y,x) d\Gamma(\mathrm{x}) + \int_\Gamma E(x) I^*(y,x) d\Gamma(\mathrm{x}) \tag{B.8}$$

The most correct function describing E^* has to be chosen, which in this case is chosen to be the fundamental solution. Assuming a concentrated charge acting at a point y, the governing equation is A.9 where Δ_y is the Dirac delta function. This solution has some useful, known properties described as A.10.

$$\nabla^2 E + \Delta_y = 0 \tag{B.9}$$

$$\Delta_y = 0 \quad for\ y \neq x$$
$$\Delta_y = \infty \quad for\ y = x$$
$$\int_\Omega E(x)\,\Delta_y d\Omega = E(y) \tag{B.10}$$

Assuming E^* is the fundamental solution to Laplace's equation gives equation A.11, and in two dimensions the fundamental solution can be expressed as A.12.

$$c(y)E(y) + \int_\Gamma E(x)I^*(y,x)d\Gamma(\mathrm{x}) = \int_\Gamma I(x)E^*(y,x)d\Gamma(\mathrm{x}) \tag{B.11}$$

$$E^* = \frac{1}{2\pi\kappa} ln \frac{1}{R}$$
$$I^* = -\frac{\boldsymbol{e_r}\cdot\boldsymbol{n}}{2\pi R} \tag{B.12}$$

From A.11, when the boundary is divided into *N* elements, the solution can be expressed as

$$c_i E_i + \int_\Gamma E\, I^* d\Gamma = \int_\Gamma I\, E^* d\Gamma \tag{B.13}$$
$$c_i E_i + \sum_{j=1}^{N} \int_{\Gamma_j} E\, I^* d\Gamma = \sum_{j=1}^{N} \int_{\Gamma_j} I\, E^* d\Gamma \tag{B.14}$$

When constant elements are evaluated, E and I do not vary within the range of integration and may be taken outside. The constant c_i can be shown to be equal ½ when the boundary is assumed to be smooth. Rearranging A.14 gives

$$\frac{1}{2} E_i + \sum_{j=1}^{N} E_j \int_{\Gamma_j} I^* d\Gamma = \sum_{j=1}^{N} I_j \int_{\Gamma_j} E^* d\Gamma \tag{B.15}$$

Everything within the integrals is known (E^* and I^* are known) and A.15 can be written as A.16 where $\widehat{H_{ij}}$ denotes the integral of I^* over element *j* with relation to node *i* and can be redefined as A.17. G_{ij} denotes the integral of E^* over element *j* with relation to node *i*.

$$\frac{1}{2} E_i + \sum_{j=1}^{N} \widehat{H_{ij}} E_j = \sum_{j=1}^{N} G_{ij} I_j \tag{B.16}$$

$$H_{ij} = \begin{cases} \widehat{H_{ij}} & i \neq j \\ \widehat{H_{ij}} + \frac{1}{2} & i = j \end{cases} \quad \text{(B.17)}$$

A.16 can then be written as

$$\sum_{j=1}^{N} H_{ij} E_j = \sum_{j=1}^{N} G_{ij} I_j \quad \text{(B.18)}$$

The complete set of equations in matrix form can be expressed as

$$\boldsymbol{HE} = \boldsymbol{GI} \quad \text{(B.19)}$$